Head-Worn Displays: A Review

Ozan Cakmakci, *Student Member, IEEE*, and Jannick Rolland, *Associate Member, IEEE*

Invited Paper

***Abstract*—Head-worn display design is inherently an interdisciplinary subject fusing optical engineering, optical materials, optical coatings, electronics, manufacturing techniques, user interface design, computer science, human perception, and physiology for assessing these displays. This paper summarizes the state-of-the-art in head-worn display design (HWD) and development. This review is focused on the optical engineering aspects, divided into different sections to explore principles and applications. Building on the guiding fundamentals of optical design and engineering, the principles section includes a summary of microdisplay or laser sources, the Lagrange invariant for understanding the trade-offs in optical design of HWDs, modes of image presentation (i.e., monocular, biocular, and stereo) and operational modes such as optical and video see-through. A brief summary of the human visual system pertinent to the design of HWDs is provided. Two optical design forms, namely, pupil forming and non-pupil forming are discussed. We summarize the results from previous design work using aspheric, diffractive, or holographic elements to achieve compact and lightweight systems. The applications section is organized in terms of field of view requirements and presents a reasonable collection of past designs.**

***Index Terms*—Head-mounted displays, head-worn displays (HWDs), near-eye display.**

I. Introduction

THE EMERGENCE of several trends, such as the increased availability of wireless networks, miniaturization of electronics and sensing technologies, and novel input and output devices is giving rise to user interfaces suitable for use in our daily living [34]. A range of displays, both on-body and in the environment, are being developed to provide visual output for the users. See [72] for a recent review of displays in the environment and [74] for an interesting instance of a projector based display. This paper will review approaches to the design of visual output devices, in particular, displays worn on the body, to support mobile users. The paper is divided into two main sections: principles and applications. The principles section(s) review the optical design and analysis techniques used in the design of head-worn displays (HWDs). HWDs are coupled with the human eye, thus, we provide a brief summary on the human visual system parameters of interest as well. The applications section is organized by field-of-view (FOV) requirements. Low-FOV designs ($<$ 40 deg), suitable for integration into an eyeglasses form factor are reviewed along with mid-FOV (between 40 and 60 deg) and Wide-FOV ($>$ 60 deg) designs. Eyeglass based displays are particularly interesting because they are well suited for mobile applications and they are more likely to enjoy higher social acceptance due to aesthetics compared to bulkier displays.

II. Principles of Optical Design for HWDs

Ideally, HWDs are designed for each specific application. Requirements of each application will guide the design process. Example specifications such as the usage of the display indoors, outdoors, or both, will determine the luminance requirement on the microdisplay. Luminance is defined as the flux per unit area per unit solid angle. Microdisplay spectrum combined with the spectral response of the human eye at the ambient illumination level of interest (e.g., scotopic or photopic) determines the spectral band of operation which can be made narrower based on the application (i.e., a monochrome display). For example, applications such as displaying thermal camera imagery may not require color displays. In order to aid in the selection of appropriate parameters for an application, there are tables available, organized by FOV, resolution, color depth, head mobility, tracking and stereo/accommodation requirements [85].

FOV is an important design specification, for example, a compact text-based display used in reading electronic mails, could be monocular and may require less FOV, whereas an immersive training application could require a stereo display with wider FOV. It is important to set the FOV based on the task and informed by the functioning of the visual pathways. However, independent of the target application all head-worn displays must meet some minimum requirements in terms of eye clearance, eye box size, image quality, and spectral characteristics. These minimum requirements are discussed in Section III.

Depending on the luminance requirements of the application, each design category can employ a laser, laser-diode, or light-emitting diode (LED)-based source in combination with a microdisplay, an organic LED (OLED) or other self-emissive display, and historically cathode ray tubes (CRTs). Average outdoors scene luminance is about 2000 fL, which is a good number to aim, and the outdoors scene luminance can be as high as 12000 fL [121]. Currently, active-matrix liquid-crystal displays (AM-LCDs), OLEDs, and liquid-crystal-on-silicon (LCOS) technologies constitute popular choices for HWD microdisplays. Liquid crystals (for example, AM-LCD or LCOS) can be transmissive or reflective [58]. OLEDs are self-emissive. OLEDs suffer not only from a shorter life span but also from nonuniform degradation of luminance for the various colors over their lifespan. The choice of OLED as the microdisplay can lead to compact HWDs compared to LCOS panels. LCOS

Manuscript received April 5, 2006; revised June 1, 2006. This work was supported in part by the Florida Photonics Center of Excellence (FPCE), by the National Science Foundation (NSF) under Grant IIS/HCI 03-07189, and by the Office of Naval Research (ONR) Virtual Technologies and Environments (VIRTE) program.

The authors are with CREOL, College of Optics and Photonics, University of Central Florida, Orlando, FL 32826 USA (e-mail: ozan.cakmakci@gmail.com).

Digital Object Identifier 10.1109/JDT.2006.879846

panels typically require illumination optics. The trade-off in using illumination optics is brightness versus compactness. OLED can be considered relatively dim compared to optimized illumination for LCOS. Compact LCOS illumination systems are an active research and optical engineering area. LED-based illumination schemes constitute one of the directions in compact LCOS illumination system development. The promise of LEDs in LCOS illumination are of a long lifespan, small physical size, and low operating voltages. LEDs can operate in sequential mode emitting red, green, and blue light at a specific time instance synchronized with the display. LED luminance is also improving and becoming suitable for low light output systems (i.e., on the order of 50 lm/W per LED). System level considerations, such as optical filters, integrators, polarization components, and projection lenses are discussed in [171], and some of these considerations apply to HWD design as well. Ferrin has compiled a more complete list of microdisplays suitable for HWD applications [83]. An in-depth discussion of microdisplay technology that covers the structure and performance of microdisplays can be found in [104].

Laser sources have been employed in scanning displays. Typically, laser-based sources have been brighter compared to their microdisplay counterparts. The perceived brightness is a function of both the laser dwell time (i.e., time allocated for the laser beam at each pixel) and the source luminance. Laser-based sources can also be divided into high and low power sources. Laser-based displays based on high power laser sources have been demonstrated with > 1500 fL luminance for military applications, however such systems are not portable and the demonstrators have been monochromatic. Laser-based displays based on laser-diodes with luminance up to 900 fL have been demonstrated for medical, aerospace, and industrial applications. An alternative to higher luminance sources is to dim the light from the scene through electrochromic or photochromic mechanisms, see [3] for an example and [43] for a review of organic and polymeric electrochromic materials.

Design trade-offs in HWDs related to the exit pupil, or eye box size which defines the limits of user eye position from which the entire display is visible, and the FOV can be understood by applying the *Lagrange invariant*. The derivation of the Lagrange invariant can be found in many classical geometrical optics textbooks, see, for example, [20]. The Lagrange invariant, axiomatically stated and applied to the pupils, can be written as follows:

$$\mathrm{LI} = n \cdot \theta \cdot y_{\mathrm{pupil}} = n' \cdot \theta' \cdot y'_{\mathrm{pupil}} \qquad (1)$$

where θ represents the semi field of view at the entrance pupil, y_{pupil} is the radius of the pupil in object space, n is the refractive index in the object space, θ' is the chief ray angle at the exit pupil, y'_{pupil} is the radius of the exit pupil, and n' is the refractive index in the image space. Using (1), for a fixed value of the Lagrange invariant, the FOV in image space is inversely proportional to the exit pupil height. A drawback of a small exit pupil is that the eye naturally moves within the display, vignetting and in a worse case scenario 100% vignetting may occur, yielding a blackout of the image. In Section IV, we will relate this property to the design of retinal scanning displays.

The light is emitted from a microdisplay, then collected by the optics within its numerical aperture, before being redistributed onto an image plane through the imaging process. The numerical aperture, or equivalently the $f/\#$ of the optics, sets the amount of light flux contributing to the imaging process. The conservation of light flux together with the Lagrange invariant now applied to the microdisplay and the image plane yield conservation of luminance. Therefore, according to the Lagrange invariant, the luminance of the virtual image formed through a HWD will be constant. The statement of constant luminance may be counter-intuitive; the common misconception is to reason that because the virtual image is magnified, the luminance would decrease. However, we need to consider both the cone angle and the magnified image plane area and remember that their product is constant.

Another fundamental trade-off in HWDs exists between the FOV and the resolution. This trade-off exists because a functionality of the HWD optics is to spread the pixels on the microdisplay across the FOV. Thus as the FOV is increased, the number of pixels per degree decreases. Approaches to overcoming this trade-off has been to use a high resolution area of interest [105], [106], resort to partial binocular overlap [82] or implement optical tiling [38].

HWDs can be monocular where a single image is presented to a single eye, biocular (see [13] for a review of biocular optics design) where the same image is presented to both eyes, or binocular where two distinct images are presented to each eye. There are optical design and perceptual issues associated with each mode.

HWDs can be designed in optical see-through, opaque, or video see-through modes. Optical see-through systems typically make use of beamsplitters to combine the computer generated objects with the real-world. In video see-through mode video cameras capture the scene which is combined with computer-generated imagery. In this mode the user views the world through the displays, therefore does not get a direct view of the world. Rolland and Fuchs compare the optical see-through and video see-through modes in [34] and conclude that the most important issues are latency, occlusion, the fidelity of the real-world view, and user acceptance. Historically, occlusion has been technically easier to achieve with video see-through display even though optical approaches to occlusion, both transmissive [66], [135] and reflective [136], [137], are actively pursued. A compact solution to the occlusion capable HWDs remains a research challenge.

View point offset is also a critical issue in systems that capture the real-world with optical systems before presented to the eyes. Magnitude of the viewpoint offset has been found to impact the sensorimotor adaptation [118]. Orthoscopic displays which do not introduce a view-point offset have been built for a modest FOV [64]. In [64] the FOV was 26×19.6 degrees. Biocca and Rolland comment that it is difficult, if not impossible, for video-based see-through HWDs to perfectly match the natural viewpoint of the user for wide FOV displays [118].

III. A Brief Summary of the Human Visual System Pertinent to the Design of HWDs

In optical design of HWDs we characterize the human visual system in terms of its object space parameters and aim to deliver a high quality image in the object space of the human eye. Designing in the object space means that we do not compensate for the aberrations of the human eye or rely on the results from the encoding and processing that occurs starting at the retina and going through the optical nerve, the lateral geniculate body, the primary visual cortex (V1), and the extrastriate areas [140]. However, a basic understanding of aberration tolerances of the eye and the influence of accommodation is useful in designing HWDs.

In this section, we shall briefly summarize some of the object space parameters of primary interest for designing HWDs. The functional primary parameters of interest are the variation in pupil size under various levels of illumination, the depth of field, the smallest feature size that the human eye can resolve, e.g., the resolution of the eye, the spectral characteristics of the light absorbed by the cones in the retina, and the aberration tolerances of the human eye. Binocular properties of the visual system which are of interest include the inter-pupillary distance and the stereoacuity which is the threshold discrimination of depth from very small disparities [59]. Finally, a summary of perceptual issues in HWDs will be provided in this Section.

The field of view of the human eye is 200 deg by 130 deg with a 120-deg overlap [121]. The lens of the eye is a gradient index element with a higher index at the center. Front focal length of the eye is about 17 mm and the rear focal length is about 23 mm, the difference is due to the fact that the refractive index of the vitreous material is 1.336 [30]. Most of the optical power is provided by the cornea. Depending on age, the lens can contribute a 10–diopter optical power change in order to focus on closer objects. There exist several optical models of the human eye, some of the more schematic but still useful models of the eye are: the reduced eye (single surface), the simplified schematic eye (three refractive surfaces), and the unaccommodated schematic eye (four refractive surfaces) [24]. The first-order parameters of interest such as the location and size of the pupil, and the center of rotation are the same across these models; therefore, they are equivalent for the design of HWDs.

The pupil is the optical aperture of the human eye which can change its size through dilation and contraction of the muscles that control the iris. The diameter of the pupil changes from 2 mm under sunlight to about 8 mm in the dark. A recent study, under ambient hospital lighting conditions (the authors do not quantify these ambient conditions), was done in 300 healthy participants and the mean resting pupil size was found to be 4.11 mm [126]. The normal eye is considered to be near-diffraction limited for a 2 mm pupil. The entrance pupil location is about 3 mm from the vertex of the cornea and resides behind the cornea [42]. Ogle and Schwartz [123] quantify that the depth of field decreases in steps of 0.12 diopters as the pupil size increase in steps of one mm.

The classical approach to determining the resolution of the eye has been the application of the Nyquist frequency to the anatomical data on the spacing of the cone mosaic. Curcio *et al.* studied the spatial density of cones and rods in eight human retinas obtained from 7 individuals between 27 and 44 years of age. An average of the center to center spacing of the cones reported in [29] yields 2.5 μm and can be converted to a visual angle of 0.5 arcmins. However, we should note that there exists studies on the cone spacing and the resolution limit reporting that, under certain conditions, observers can see fine patterns at the correct orientation when viewing interference fringes with spatial frequencies as much as about 1.5 times higher than the nominal Nyquist frequency of the underlying cone mosaic [28]. Currently, the trend in HWD design is to aim for 1 arcmins of visual acuity. We should also note that the higher visual acuity occurs within the fovea region, spanning roughly ± 5 deg around the optical axis of the eye. Finally, dynamical visual acuity [32], while challenging to measure, is of critical importance to HWD design. It is well known that the human visual system summates signals over a time period of about 120 ms. In quantifying visual performance for moving factors, a compounding factor is motion smear. Burr reports that if the target is exposed long enough the amount of smear is far less than may be expected [172].

Stray light, caused by ocular scattering, affects the contrast specification of an HWD [76]. De Wit shows that for a 24×18 deg display, the maximum achievable contrast for a 4×4 checkerboard image is approximately 80:1. This is calculated by convolving the ideal image with the point spread function of the eye. Hasenauer and Kunick analyzed the impact of veiling glare in an HWD system and offered techniques to isolate the sources of stray light and minimize their impact in the design [107].

Spectrally, light is transmitted starting at about 400 nm and up to 1400 nm through the ocular media [25]. However, only a selected portion of these wavelengths are absorbed by the cones, depending on the level of illumination. Based on the Commission International de L'Eclairage (CIE) curve, we can consider the photopic visible spectrum to span from 400 to 700 nm. The photopic response curve peaks at 555 nm. Based on the photopic response curve, optical designers choose a spectral weighting scheme and incorporate it as a meaningful factor throughout the optimization process.

Burton and Haig [47] simulated the effects of Seidel aberrations (defocus, spherical aberration, astigmatism and coma) on four images and determined the tolerances of the human visual system to different levels and combinations of the aberration types by a forced-choice discrimination task [50]. The basic idea in the experiment is to convolve targets with aberrated point spread functions having varying levels of aberration and to compare the aberrated image against the original in a controlled setting to quantify the level of just-noticeable differences between the images. Measurements of aberration tolerances were performed with 2 mm pupils. A summary of the averaged peak to valley aberration thresholds for 60%, 75%, and 90% discrimination probabilities, across four targets and two observers is given in Table I.

In terms of chromatic aberrations of the eye, Rodgers calculated the chromatic aberrations of the eye by combining the photopic response curve with the chromatic aberration curve of the eye and found an error of $\lambda/4$ for a pupil of 2.4 mm [101]. Hence, the chromatic aberration of the eye under photopic conditions, for an average outdoor scene, is rather benign. Mouroulis *et al.* [162] reported that the 2.5 arcmins recommendation represents a measurable drop in performance and constitutes a realistic tolerance for the transverse chromatic aberration.

Binocular properties of the visual system are important for all modes of operation monocular, biocular, and binocular displays. Briefly, with monocular displays the visual system in many cases may respond with binocular rivalry, a perceptual

TABLE I
ABERRATION THRESHOLDS IN THE FORM OF JUST-NOTICEABLE DIFFERENCES LISTED IN TERMS OF PROBABILITY OF DISCRIMINATION

Peak to Valley Wavefront Aberration (in units of Wavelengths)			
	60%	75%	90%
Defocus (W20)	0.14±0.013	0.22±0.016	0.3±0.019
Spherical (W40)	0.13±0.013	0.21±0.013	0.29±0.014
Astigmatism (W22)	0.20±0.017	0.30±0.019	0.41±0.023
Coma (W31)	0.30±0.02	0.46±0.031	0.62±0.045
Strehl Intensity Ratio			
Defocus	0.93±0.013	0.85±0.022	0.73±0.031
Spherical	0.94±0.012	0.86±0.017	0.77±0.02
Astigmatism	0.92±0.017	0.80±0.023	0.68±0.027
Coma	0.95±0.006	0.89±0.015	0.81±0.026

conflict when the two eyes receive very different stimulation. With biocular displays, the two eyes receive the same stimulation which would signal to the visual system that the scene contains zero disparity throughout the visual field (which would dilute the visual effect of any perspective depth cues present) [173]. See [51] for a discussion of binocular issues associated with the design of stereo displays. A review of human stereopsis is provided by Patterson and Martin [59], readers interested in depth perception in stereoscopic displays may also refer to [119]. Patterson organizes his review around five functional topics that may be important for the design of stereoscopic display systems: geometry of stereoscopic depth perception, visual persistence, perceptual interaction among stereoscopic stimuli, neurophysiology of stereopsis, and theoretical considerations. Important concepts in stereopsis stem from the retinal positions of images referred to as disparity. The horopter can be thought of as a baseline of zero disparity based on the retinal images, and can be defined geometrically (Vieth-Muller circle) or psychophysically [59]. In terms of the geometry of stereoscopic depth perception, Patterson notes that the processing for points inside (crossed disparity) or outside (uncrossed disparity) of the horopter is done by separate mechanisms [60]. The consequence is that depth perception quality can be different for points residing in the crossed and uncrossed disparity regions. The small area slightly in front or behind the horopter is called the *Panum's fusional area*. In terms of binocular fusion, fusion limits depend on the disparity magnitude. Fusion limits are given to be 10 arcmins (e.g., small disparity), 2 deg (e.g., medium disparity) and 8 deg (e.g., high disparity). Beyond these limits, objects may be seen double (diplopic). The disparity limits of fusion are reported to covary directly with stimulus size or scale, and inversely with spatial frequency. The limit does not vary with contrast. Vergence eye movements are known to improve the range of disparities that can be processed by the human visual system. Clinical tests carried at a distance of 40 cm with a fixed 65 mm IPD assumption yield a stereoacuity between 20–40 arcseconds [25] and stereoacuity can be as low as 8 arcseconds [59]. It is known that stereoacuity varies with luminance and spatial frequency [60]. Patterson found that high stereoacuity is obtained with high spatial frequencies and low temporal frequencies [174]. High stereoacuity is achived in the fovea region. Therefore, high quality depth discrimination over the visual field requires eye movements [59]. The optical design consequence of supporting eye movements is to have either a large exit pupil or eye tracking capability [166], [168]. The optical consequences of eye movements in visual instruments include full or partial vignetting and was analyzed in [62]. In terms of visual persistence, Patterson and Martin [59] recommend that for displays operating using the field sequential technique, longer durations of 10 ms or higher would be expected to produce better depth perception due to greater binocular integration for each channel. Other trade-offs such as color smear will need to be investigated.

According to MIL-STD-1472C and the literature on the statistics of IPD values including, the IPD adjustment range for a binocular HMD is recommended to be at least 50–78 mm. U.S. Air Force anthropologists measured the IPD of 4000 flying personnel and the mean yielded 63.3 mm [114]. Self provides a review of optical tolerance limits for binocular displays [56]. Based on the rather sparse data available in this field, recommendations of Self are based on studies of Gold [133] and Gold and Hyman [134]. Both of these studies are limited to no more than four observers, hardly representative of a population as noted by Self. Self recommended vertical misalignment of the two optical axes, horizontal misalignment of the two optical axes, rotational difference between the optical axes to not exceed 3.4 arcmins. Self recommended that the tolerance for the magnification difference between the two images at the edge of the overlap area to not exceed 10 arcmins with a less than 3.4 arcmins preferred value. Self recommended a luminance difference tolerance between the two images to be less than 25% and preferably less than 10%. Self recommended the collimation tolerance shall be such that the optical distance to the displayed image shall be between 100 m to ∞.

Patterson, Winterbottom and Piece provided a comprehensive review of perceptual issues in HMDs [122] which we shall summarize in this paragraph. Patterson organizes his review in five sections: luminance and contrast and their effect on depth of field, dark focus and dark vergence, accommodation-vergence synergy and its effect on perceptual constancy (e.g., size and speed constancy), eye strain and discomfort, FOV and its relationship to the functioning of different visual pathways, binocular input and its relationship to visual suppression and head movements.

In terms of luminance and contrast, as the luminance is increased, the pupil size reduces and the depth of field increases. The competing trend is that as the target resolution increases, depth of field decreases. Therefore, both the luminance level and the target resolution should be considered when designing for a specific depth of field value. Depth of field is a critical distance that determines objects that appear in sharp focus. Depth of field should be set appropriately so that the user can properly perceive both the computer generated imagery and the real objects lying at the same depth. Under low levels of illumination or degraded stimulus conditions, the accommodation will rest around a 1 m value with some variation [124].

The human eye has evolved in such a way as to converge and accommodate at the same point of interest as it saccades across the FOV. Monocular systems can present the magnified virtual image of the microdisplay at a fixed distance from the user and the information appears to reside on this single plane. The consequence is that the users can accommodate and converge on the plane of the virtual image which is consistent with the accommodation and convergence mechanism of the human eye. Stereo displays demand that the users focus on the plane of the virtual images formed by the optics and converge potentially at different depths away from that plane in order to perceive three dimensional. As a guideline, the human eye requires that accommodation and convergence match to within ± 0.1 of a diopter [36]. Accommodation and convergence conflict is known to result in eye strain and discomfort. Moffitt reports a $+ - 0.25$ diopter to be workable and a ± 0.5 diopter as the maximum level of mismatch [37]. If the accommodation and convergence planes are further apart than the workable mismatch, the eyes would converge to the correct location to avoid diplopia and suffer from excessive blur as a trade-off. Multi-focal displays have been proposed to resolve the accommodation-convergence conflict [38]. When the accommodative response becomes a compromise between the stimulus and the dark focus value, size, depth and speed may be misperceived. Vergence seems to be valid down to 0.02 fL [127] and the accommodation seems to be valid down to between 2–100 fL [125]. In terms of the accommodation-vergence conflict, Patterson recommends that more research is necessary to determine the exact tolerance limits.

Multi-focal planes could be based on non-moving parts. The idea in multifocal planes is to construct a miniature 3-D display, image the 3-D source into a volume perceived as continuous dictated by the limits of human visual acuity. The natural question to ask is the minimum number of planes one would need to cover the whole visual space. Rolland *et al.* has shown that 14 planes can cover a focusing distance from 0.5 m to infinity, under the assumptions of a 4-mm pupil and a 1-arcmins visual acuity [38]. When considering moving parts, Wann proposed tracking the eye and coupling eye movements to adjust the image plane depth via a servo-lens mechanism [51]. Alignment of the optics for each eye is a critical issue in stereo displays.

In terms of field of view, the human visual system seems to process two cortical streams [127]: Dorsal stream, which connects the central and peripheral retinal areas to the magnocellular pathways, and seems to be responsible for optical flow processing as well as visuomotor abilities such as reaching. The dorsal stream processes low spatial frequency and high temporal frequency information. The ventral stream, connects mainly the central retina to the parvocellular pathways which are responsible for high spatial frequency and low temporal frequency information processing as well as color. For tasks such as targeting and object recognition, processed through the ventral stream, a FOV of 50 deg can be sufficient. For tasks requiring peripheral stimulation, Patterson recommends greater than 60 deg. The perceptual trade-off in wider field of view is between the level of immersion and nausea.

References [46], [122] provide a discussion of visual issues in the use of a head-mounted monocular display. The monocular, partially occluded mode of operation interrupts binocular vision. Moreover, presenting disparate images to each eye results in binocular rivalry. Peli recommends using a peripheral positioning in order to maintain normal binocular vision of the environment. Peli also notes that under conditions of rivalry, the brighter field will dominate. Display resolution and contrast are reported to be of secondary importance for rivalry. In a recent study Sheedy and Bergstrom [138] performed a text-based task comparison of five displays: monocular virtual, binocular head-mounted virtual, hard copy, flat panel, and a small format portable display. Performance speed on a monocular HWD was found to be comparable with performances on flat panel and hard copy. Interestingly the authors found that the performance speeds on the binocular HWD were about 5% slower than normalized performances, 6.75% slower compared with the traditional flat panel and hard copy displays. The authors also report that the symptoms of eyestrain and blurry vision were significantly higher on monocular HWDs than on other displays.

Finally, a key perception issue of binocular HWDs is the quantification of depth perception. While there is a large body of literature relating to depth perception, for example Cormack [175], Fox and Patterson [176], Becker *et al.* [177], some of the earlier works that studied depth perception in see-through HWDs were conducted by Ellis [67] and Rolland [169]. In his work, Ellis quantified the accuracy and precision of perceived depth for real and virtual objects, where the real objects included some surface in front or behind the virtual objects. Results showed that under the observation conditions some bias in depth perception was measured. Rolland in a first study investigated the accuracy and precision of perceived depth for two real, two virtual, and one real and one virtual objects side by side. No bias was measured for the two first cases in spite of having the 3-D objects displayed at either 0.8 or 1.2 m while the optical images were collimated. For the real/virtual condition a bias of about 30 and 50 mm for 0.8 and 1.2 m was reported. The study pointed to the dificulty in presenting virtual objects at targeted precise depths and the need for optimized methodology. In recent work, Rolland revisited aspects of the methodology to quantify depth perception in HWDs and concluded that the method of adjustments with two stimuli of different shapes was most appropriate [170].

IV. Pupil-Forming Versus Non-Pupil-Forming Designs

It is possible to categorize optical designs for HWDs into pupil forming and non-pupil forming. Pupil-forming designs include eyepieces that magnify an intermediary image while imaging the pupil of the optical system forming the exit pupil, projection optics, and retinal scanning displays which can optically be considered as scanning projection systems. Non-puforming designs include magnifiers. The optical systems designed for HWD applications fall into two broad design form categories: magnifier/eyepiece based designs and projection based designs. Once a microdisplay suitable for the task is chosen, the role of the optical system is to relay a magnified virtual image of the microdisplay to the human visual system. The gain in apparent size is typically quantified by comparing the image seen through the lens to the image seen with the unaided or naked eye. For the unaided human eye, the apparent size of a microdisplay can be increased by bringing the microdisplay closer to the eye up to the accommodation limit. Compact and lightweight optical systems are necessary in many applications, especially when the users are mobile. Compactness of the microdisplay necessitates a magnification

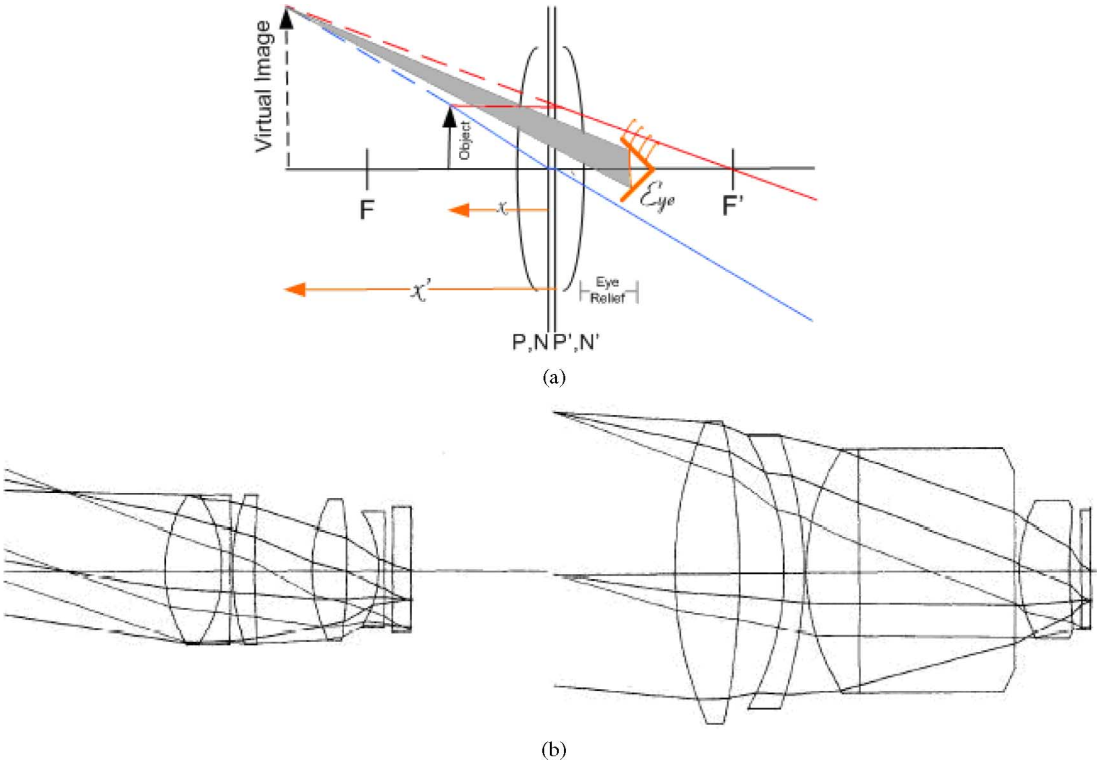

Fig. 1. (a) Geometry of a *magnifier*. A magnifier forms a virtual image and the observer's pupil becomes the exit pupil of the system. The distance from the vertex of the last physical surface of the system to the exit pupil is called the eye relief. (b) Example 45-mm focal length magnifiers. Monocular (left) and biocular (right). Both systems are working with a 30-mm screen diameter. The monocular system has a 40-mm 'exit pupil' and the biocular system has an 84-mm 'exit pupil', the latter being large enough to cover both eyes. (Adapted from Williamson [24]). (Color version available online at http://ieeexplore.ieee.org.)

requirement since the microdisplay typically is too small to view with the unaided eye.

Regardless of complexity (i.e., types or number of surfaces), an optical system can always be characterized by an effective focal length along with principal planes and nodal points. A *magnifier* forms a virtual image when the object lies inside of its focal length, as shown in Fig. 1. Distance x is the object distance and it is measured from the principal plane P. Distance x' is the image distance and it is measured from the principal plane P'. We assume the object and image spaces to reside in air, therefore, the nodal points (N and N') are at the same points as the principal planes. The formation of the virtual image is illustrated by tracing an off-axis ray through the nodal point and a ray parallel to the optical axis of the system, the intersection point of these rays determine the location and size of the virtual image. The virtual image formed by a magnifier has the same orientation as the object—sometimes referred to as erect in the optics community. In HWDs, the virtual image can be placed within about 1 m for near-field tasks or beyond 1 m for far-field tasks. Optical distances can also be measured in diopters which is a reciprocal of the optical distance expressed in meters. The pupil of the observer becomes the limiting aperture and the exit pupil in a magnifier. Magnifiers are typically designed to accommodate a range of eye movements such as translations and rotations while observing the virtual image formed by the magnifier. The eye motion requirement combined with a desire to achieve good image quality motivates designs more complicated than a single lens. In terms of image quality, we desire that the points in the object map to points in the image, as limited by the size of the pixel or the resolution of the eye, planes map to planes and that the desired magnification remains constant across the image. Deviations from these desires are called *aberrations* and it is the task of the optical designer to minimize them.

As an example of noncollimated single lens magnifier, Coulman and Petrie [113] discuss the design of a binocular magnifier with a conic surface. They compare the shapes and relative positions of images formed for each eye through a binocular magnifier with spherical surfaces and another magnifier combining a spherical and a conic surface. For each line of sight of each eye, there will be an astigmatic focus, different for the tangential and the sagittal directions. The middle point between the tangential and the sagittal surfaces can be taken as the focus surface, which is not necessarily the convergence surface. Therefore, the magnifier based on spherical surfaces creates images considerably different for each eye which requires the eyes to fuse two completely different images, especially toward the edge, leading to a disturbance of the accommodation and convergence relation. Rogers and Freeman reoptimized the design given by Couldman and Petrie to have a diameter of 79 mm and having a sixth-order aspheric surface and they reported a magnification of 2.3× [112].

An *eyepiece*, in addition to creating a virtual image for the human visual system, forms an exit pupil by imaging the pupil of the system prior to it to the image space. The distance between the edge of the last surface and the exit pupil is referred to as *eye clearance*. The distance from the vertex of the last surface to the exit pupil is called the *eye relief*. A minimum eye clearance distance is considered to be 20 mm according to Kocian [17] as well as Self [56]. Self [56] recommends the minimum exit pupil size of an HWD to be 10 mm. In the case of a telecentric design, the eye relief distance determines the focal length of an eyepiece. One might think that since the light cones for various fields have the same angles in the image space for a telecentric design, the consequence would be uniform illumination. However, Reiss shows that the illumination varies with the obliquity of the entering light [163]. In a telecentric lens, as the field angle increases, the height of the lens will scale accordingly causing an increase in weight. HWDs with relaxed telecentricity conditions have been built successfully [41].

For compact and telecentric systems, the designers goal is to optimize the design for a specific eye relief distance and have it as close as possible to the focal length. In a recent study, we compared two eyepieces: one closely resembling an Erfle eyepiece and a second one where the doublets in the Erfle-like eyepiece were replaced with diffractive optical elements. We quantified that the eyepieces having diffractive optical elements can support an eye relief range of about 80% of their focal lengths, much higher than the doublet based system. In terms of FOV, 30 degrees is typical for simpler eyepieces while higher fields of view with considerable aberration correction have been achieved. The Scidmore eyepiece [18] may be considered for a 72-deg example and the Dilworth eyepiece [19] for a 90 deg example.

The aberrations of interest in eyepiece designs are lateral color, spherical aberration of the pupil, distortion, field curvature, and astigmatism. In the case of HWDs, some amount of distortion in the optics can be accepted as it is possible to correct distortion by prewarping the images on the microdisplay in hardware or software or optically [91], see [34] for an example. In wide angle eyepiece designs 8%–10% of distortion is considered typical [131]. If the distortion is to be corrected in electronics, it is crucial to achieve real-time correction ($<$ 10 ms delay per frame). Spherical aberration of the pupil refers to the change in the exit pupil position with field angles. Spherical aberration of the pupil is closely linked to distortion [131]. Distortion can be defined as nonlinear magnification across the field of view. The consequence of forming an exit pupil outside of the eyepiece is broken symmetry about the pupil. Broken symmetry makes aberration control challenging.

Aberrations of magnifiers are different from those of eyepieces. For example, in a magnifier design, the eye is allowed to move considerably more compared to a pupil forming eyepiece, therefore, aperture size dependent aberrations such as on-axis spherical, oblique spherical and all orders of coma become more challenging to correct [24].

Head-worn optical projectors are an alternative optical design form to the eyepiece based designs. The basic idea in an optical head-worn projector is to place the microdisplay outside of the focal length of the projection lens in order to form a real image in front of the user. The real image formed by the projection lens can be displayed on a diffuse [71] or a retroreflecting screen [41]. An account of conventional projection screens can be found in [79]. A retroreflecting screen eliminates optical crosstalk between users and allows for multiple users to interact within a virtual environment. A retroreflecting screen also maximizes light throughput compared with a diffused

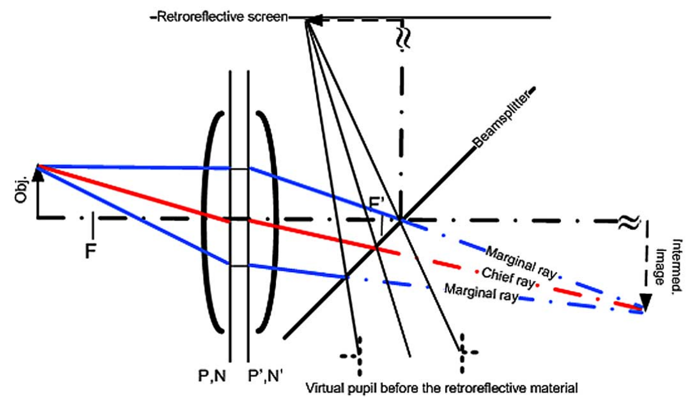

Fig. 2. Optical layout of a head-worn projection display. (Color version available online at http://ieeexplore.ieee.org.)

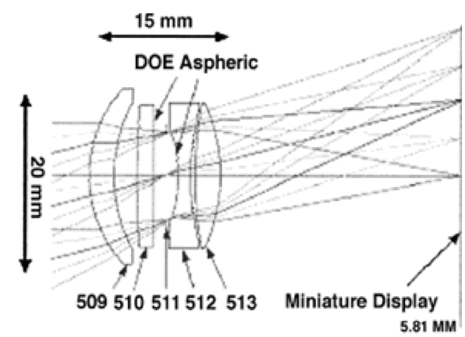

Fig. 3. Modified double-Gauss head-mounted projector example. (Adapted from [41]).

screen. The retroreflecting screen can be placed physically or optically in the environment depending on the application. Optical placement allows for using the display outdoors, eliminating the requirement to have a screen physically placed in the environment [164].

The optical path in a head-worn projector with an external retroreflective screen is folded using a beam splitter to direct it towards the screen placed in front of the user. The retroreflective screen will direct the light back, at least in principle, exactly in the same direction when the light meets the retroreflective screen. An example optical layout for the HMPD is shown in Fig. 2.

Optical projectors based on a modified double Gauss lens form have been designed. The optical layout of a modified double-Gauss lens for a head-mounted projector application if shown in Fig. 3. Double-Gauss designs decend from the double meniscus anastigmat lenses [131]. Double-Gauss lenses can achieve a flat field by balancing the positive and the negative surfaces. Symmetry around the pupil in the double-Gauss form helps with aberration correction. Double-Gauss lenses are limited by oblique spherical aberration caused by the anamorphism seen by the bundles at maximum field angles as they pass through the lens [132]. It is well known that systems exhibiting symmetry about the pupil will have all odd aberrations minimized, such as coma, distortion and lateral color. In an HMPD, the pupil resides within the optical system, symmetrically, and can be conjugated to the eye through the beamsplitter forming a virtual pupil [164]. Such designs allow large fields of views without any significant scalability in the optics, thus yielding wide angle compact designs.

Retinal scanning displays (RSD) aim to scan a beam of light onto the viewers retina. The early prototypes developed in the 1990's used lasers and acousto-optic modulators to implement the retinal scanning concept [52]. Different scanning techniques such as rotating polygons, galvanometers, piezoelectric deflectors, acousto-optic deflectors, have been compared by Holmgren and Robinett [5] in terms of resolution, sweep frequency and cost. Based on the commercially available scanning techniques of the time, Holmgren and Robinett concluded that none of these scanning technologies promised a display system that would be clearly superior to current CRT and LCD displays in HMD applications. Recent work on the design of MEMS scanners shows that it is possible to design and fabricate MEMS scanners that can operate at frequencies high enough to support 1280×1024 resolution. A comparison of thirteen state-of-the-art scanners published in the literature is provided in [115]. De Wit designed, implemented and assessed a retinal scanning display based on a scanning polygonal mirror. De Wit points out the interesting similarity between the retinal scanning devices and the scanning laser opthalmoscopes which can be regarded as the predecessor of the retinal scanning devices [4]. Recent efforts in RSD development have focused on miniaturizing and analyzing the micro-electro-mechanical scanners (MEMS) [53].

At the system level, the building blocks of retinal scanning displays can be broken down into video electronics, a photonics module, a scanner module, an exit pupil expander, and a viewing optic. In the following paragraphs, we will summarize the functionality of each module and the interested reader should refer to [54], [75] for further details and references.

Based on the desired video signal input, the video electronics module controls the intensity and the mix of colors in the photonics module and generates the time-synchronized control signals for the scanner module. For each pixel, the photonics module is responsible for delivering a light beam to the scanner module with the desired intensity and color as requested by the input video signal. In LED or laser-diode based systems pixel intensity can be controlled directly by varying the drive current. The alternative to direct modulation is to use an external modulator such as an acousto-optic or an electro-optic modulator. Luminance control can be implemented as a separate module if necessary, for example, in the form of polarizers, fiber-optic or electro-optic attenuators. In principle, given a fast modulation scheme, it should be possible to adjust the convergence for each pixel, therefore, imposing depth on each pixel [77].

The scanner module is responsible for directing the beam of light delivered from the photonics module to the desired image plane location. Relying on persistence of human vision, it is the fast and repeated scanning onto the retina that creates the perception of a static 2-D image. A number of scanning methods exists; for example, polygonal scanners, oscillatory scanners, acousto-optic and electro-optic scanners, and holographic scanners. There are several ways to implement scanners and biaxial MEMS scanners have been fabricated for use in commercial products by Microvision. In a biaxial MEMS scanner, the mirror is suspended with two flexures in a gimbal and is actuated via electrostatic plates under the mirror. Diffraction limited performance requires the scan mirror to be optically flat ($\lambda/10$). Pixel location and luminance variations caused by nonlinearities in the scanning can be overcome by synchronizing the output based on a look-up table that accounts for the nonlinearities.

In order to create a comfortable eye-motion box, a 10–15-mm exit pupil is preferred. However, without exit pupil expansion, a typical exit pupil size in RSD systems is reported to be 1–2 mm as imposed by the Lagrange invariant discussed in Section II. Therefore, for improved usability and to accommodate positioning error, it is essential to use an exit pupil expander unless the system makes use of an eye tracker and moves the exit pupil accordingly.

In laser-based RSDs, a Gaussian beam propagates through the scanner optics and forms a Gaussian spot, therefore, beam truncation impacts resolution and contrast [1]. For a detailed discussion on fundamental work in imaging with Gaussian pupils, see [2].

A light emitting diode (LED) based scanner has been designed by Wells and Becker [45] as shown in Table II. In this system, LEDs, a magnifying lens which forms a virtual image, and a vibrating mirror are employed to scan a few rows at a time. The imaging optics is designed for adjustable focus. This display provides 720 (H) $\times$ 480 (V) pixels across a $21^\circ \times 14^\circ$ FOV. The display is monochromatic which makes the magnifying optics simpler since achromatization is not necessary.

V. Applications of Aspheric, Diffractive, Holographic and Freeform Surfaces in HWDs

In spite of cost, difficulties in fabrication and testing, and a deficiency of less than 100% light throughput in the case of diffractive and holographic surfaces, freeform [158], diffractive [8], [10] and holographic surfaces have been used successfully in previous HWD designs [12], [81], [84], [93], [129].

The main use of diffractive optical elements is rooted in their ability for color correction, specifically, their approximately -3.5 Abbe number which provides complimentary dispersion characteristics when used with optical glasses and plastics; Stone and George [48] present a nice derivation of this fact. It is possible to replace the doublets used in color correction with diffractive optical elements yielding weight reduction. Missig and Morris point out in [120] that as the task of color correction is shifted to the diffractive optical element, the steep curvatures for negative color correction elements reduce leading to reduced aberrations. Details of aberrations inherent in the diffraction process can be found in [165].

The contours of diffractive optical elements can be fabricated in discrete steps using lithographic techniques, diamond turning, laser writing as well as electron-beam lithography. Therefore, the minimum feature size becomes an important parameter in the utilization of diffractive optical elements as constrained by the fabrication methods. Sub-micron (0.1 μm) feature sizes have been demonstrated [43]. Many diffractive elements are based on plastic materials for their substrate. Popular plastic materials include acryclic (PMMA), Styrene, NAS, SAN, polycarbonate, tpx, abs, and nylon. Materials choices are limited in plastics compared to glasses. Injection molding and compression molding processes make volume manufacturing feasible for plastic optics. Aspheric surfaces can

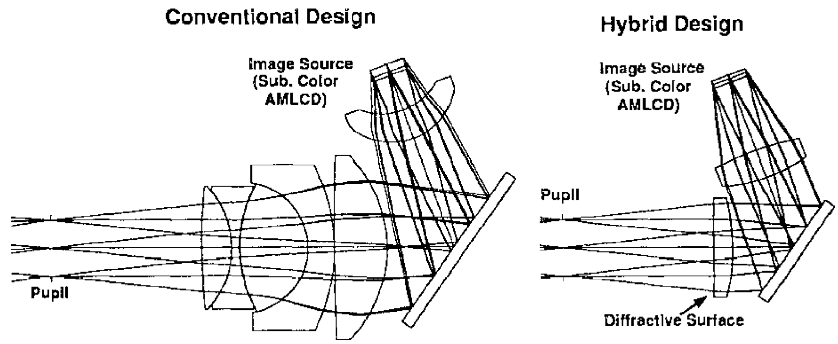

Fig. 4. Comparison of a conventional and a hybrid design using diffractive optical elements.

be manufactured on plastic by diamond turning and rms surface roughness of less than 50 Å can be achieved.

A concrete comparison between a pure refractive solution and a hybrid refractive-diffractive design has been provided in [8] by Cox *et al.* and the systems compared are shown in Fig. 4. Fig. 4 shows two systems having equivalent optical performance. Each system is reported to have a 15-mm exit pupil, 20-deg FOV, and a 75% diffraction limited modulation transfer function (MTF) at the Nyquist frequency of the display for the visible spectrum. The design using diffractive optical elements has only two elements and is reported to weigh ten times less than the conventional design.

A second example is given by Stone and George [48]. These authors study in detail hybrid lenses with diffractive and refractive elements and show that two and three wavelength achromats can be achieved with smaller refractive curvatures at larger attainable apertures. The authors also point out the capability of hybrid elements to achieve an Abbe number ($V = nd - 1/nf - nc$, where nd, nf, and nc are the refractive indices of the D (587.6 nm), F (468.1 nm), and C (656.3 nm) lines, respectively) of arbitrary value.

A third example, utilizing diffractive–refractive optical elements, discussing the relationship between the MTF and the diffraction efficiency is provided in [15], based on a relay lens system. The authors compared a plano–convex refractive element against a plano-convex with a diffracted optical element. This study reports the integrated diffraction efficiency of the hybrid element to be 91% and concludes that the effect of the wavelength dependent diffraction has little impact on the imaging performance. The authors use the modulation transfer function as their criteria for image quality comparison between the hybrid and the pure refractive element.

A fourth example is the design by Missig and Morris [120], where the authors designed hybrid elements with $>$ 60 deg FOV and reported a 70% weight reduction compared with the Erfle eyepiece as well as a 50% decrease in the pupil spherical aberration and a 25% reduction in distortion.

A fifth example is provided by Knapp *et al.* [31] where the authors compared an eyepiece using a diffractive optical element to an eyepiece using aspheric elements. The system in in [31] uses spherical glass elements and a diffractive surface compared with a system that uses spherical glass elements and a plastic aspheric element. The development criteria for the lenses was a 60-deg full FOV, 24-mm focal length, 10% distortion, 12-mm exit pupil and a 20-mm eye relief over the 540–558-nm spectral band. Aberration tolerances were ± 2 D on the focus range, ± 0.25 D on the field curvature, < 0.5 D for astigmatism. There were additional packaging constraints as well. They draw the conclusion in their study that the diffractive optical element yields a better optical design from a chromatic, field curvature and MTF standpoint for their set of specific application requirements.

Due to multiple diffracted orders, power in orders other than the one a designer is using serves to reduce the contrast in the final image. Buralli and Morris define a quantity called the integrated efficiency which serves as a useful figure of merit to describe diffractive lenses [22]. Missig and Morris [120] note that numerous factors can affect the diffraction efficiency, including the surface blaze profile, the zone spacing, the surface coatings, the illumination wavelength, the incidence angle, the polarization, and the substrate index of refraction.

The use of holographic optical elements [14] is motivated by aberration correction, suitability in off-axis geometries, applicability to semi-transparent optical combining, and compact and light packaging requirements. The disadvantages of holographic elements include their low efficiency across a broad spectrum. Ando *et al.* [84] experimented with a holographic combiner which can transmit the rays from the scene and reflect a narrow band of specific wavelengths. The authors used a single HOE of 4” × 5” size and recorded two beams incident at 30 deg, one for each eye, in order to generate the necessary parallax per eye from a single HOE. A He–Ne laser (632.8 nm) was used in the recording process and a semiconductor laser (635 nm) was used in the reconstruction process. Finally, the use of volume hologram written in the UV part of the spectrum but replayed in the visible part of the spectrum were explored towards use in HWDs [93]. The promise is more efficiency as compared to surface holograms.

VI. Applications of HWDs: Low FOV Designs ($<$ 40 deg)

> “Wearable computing allows graphics and text to be associated with physical objects and locations. Through overlay displays, the user can concentrate on the task instead of constantly looking down as is the case with notebook computers or pen-based systems. Techniques are available to sense what object the user is looking at, the computer may deduce the user’s intention and update the display automatically.” [78]

TABLE II
LOW FIELD-OF-VIEW DESIGNS (< 40 deg)

Spitzer. Eyeglass Display Lens System Employing Off-Axis Optical Design.
US 6,353,503
Mar. 5, 2002

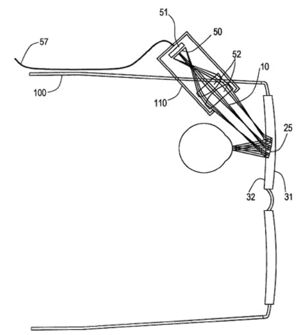

(a)

Bettinger. Spectacle-mounted ocular display apparatus.
US 4,806,011
Feb. 21, 1989

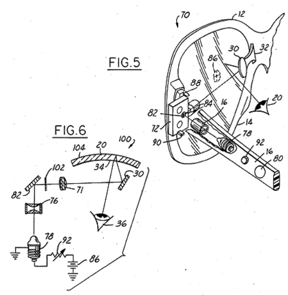

(b)

Hoshi *et al.* Off-axial HMD optical system consisting of aspherical surfaces without rotational symmetry.
In Proc. of SPIE Vol. 2653

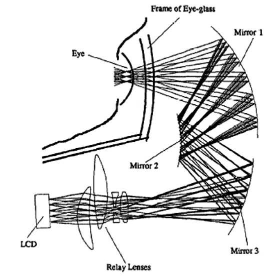

(c)

Perera. Display Projection Optical System for Spectacles or Sunglasses.
US 4,867,551
Sep. 19, 1989

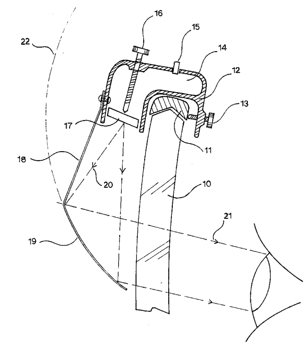

FIG. 2

(d)

Mann. Wearable Camera System With Viewfinder Means.
US 6,307,526
Oct. 23, 2001

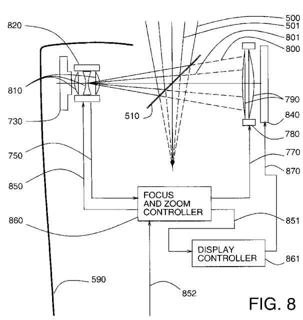

(e)

Geist. Head-mounted virtual display apparatus with near-eye deflecting element in the peripheral field-of-view.
US 6, 771,423
Aug. 3, 2004

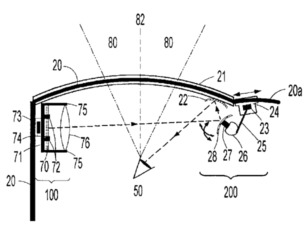

FIG. 2

(f)

Amafuji. Head Mounted Display Device.
US 6,359,602
Sep. 19, 2002

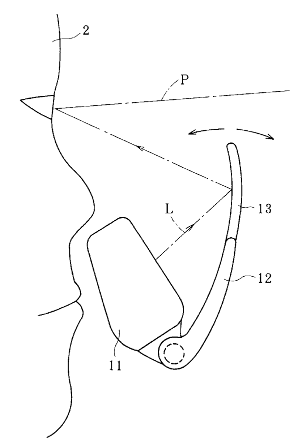

(g)

Kuriyama. Image Display Apparatus
US 6,081,304
Jun. 27, 2000

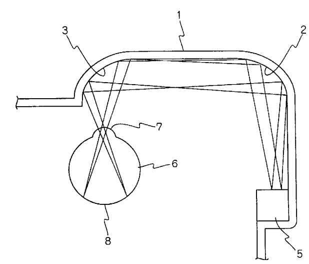

(h)

Pekar. Vision enhancing system.
US 4,704,000
Nov. 3, 1987

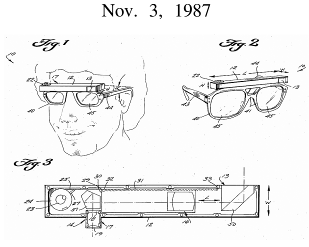

(i)

Togino. Prosm Optical System.
US 5,991,103
Nov. 23, 1999

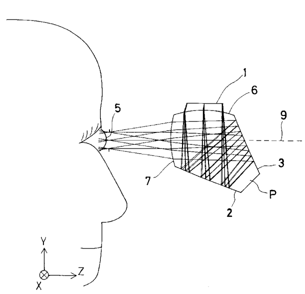

(j)

Furness. Display System for a Head Mounted Viewing Transparency.
US 5,162,828
Nov. 10, 1982

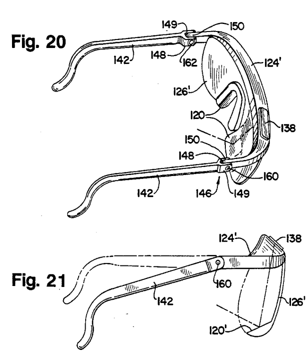

(k)

Holakovszky. Stereoscopic video image display appliance wearable on head like spectacles.
US 5,129,716
Jul. 14, 1992

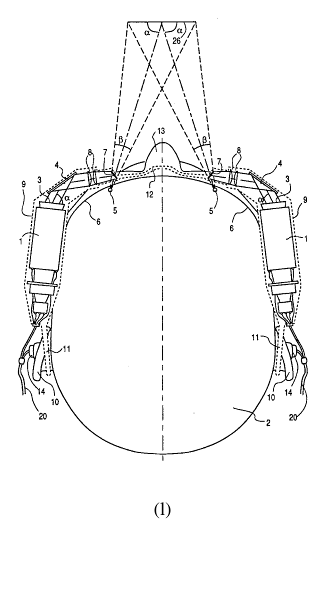

(l)

TABLE II *(Continued)*
LOW FIELD-OF-VIEW DESIGNS (< 40 deg)

Iba. Image Observation Device.
US 5,384,654
Jan. 24, 1995

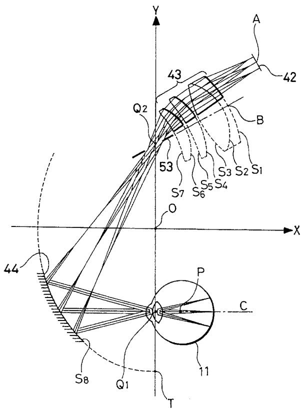

(m)

Kubik. Headwear-mounted
Periscopis Display Device.
US 4,753,514
Jun. 28, 1993

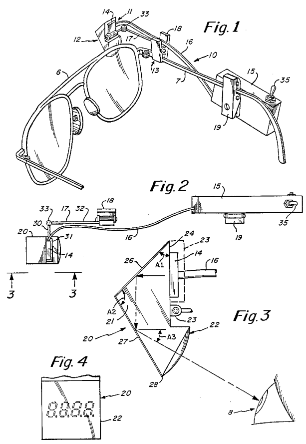

(n)

Ferrin. Headgear Display System
Using Off-axis Image Sources.
US 5,576,887
Nov. 19, 1996

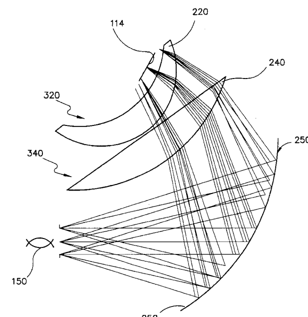

(o)

Lippert. Visor Display with
Fiber Optic Faceplate Correction.
US 5,309,169
May 3, 1994

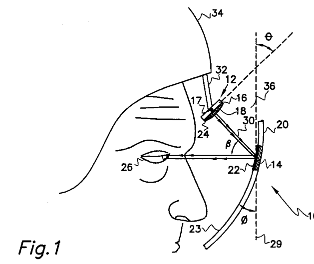

(p)

Lacroix. Device for the Display
of Simulated Images for Helmets.
US 5,184,250
Feb. 2, 1993

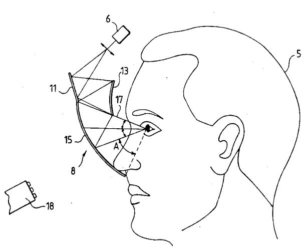

(r)

Kasai. A Forgettable Near-Eye Display.
ISWC 2000

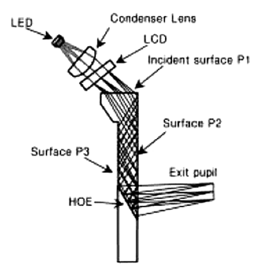

(s)

Bosserman. Toric reflector display.
US 4,026,641
May 31, 1977

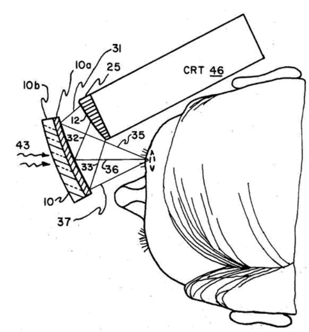

(t)

Nagaoka. Light weight head
mounted image display device.
US 6,697,200
Feb. 24, 2004

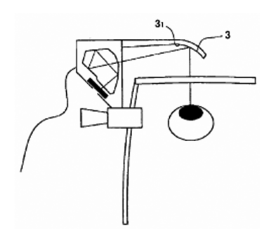

(u)

Takeyama. Observation optical system.
US 6,710,902
Mar. 23, 2004

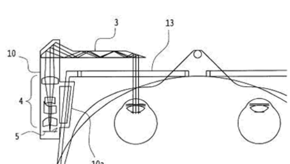

(v)

Song. Wearable display system.
US 6,882,479
Apr. 19, 2005

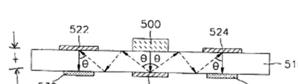

(w)

Robinson. Video headset.
US 5,696,521
Dec. 9, 1997

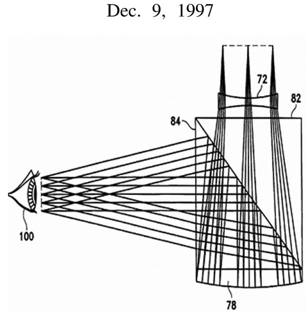

(x)

Fritz. Head mounted display
using mangin mirror combiner.
US 5,838,490

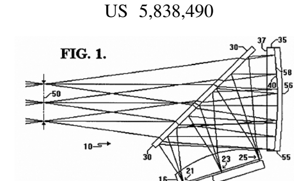

(y)

TABLE III
MID-FOV DESIGNS (BETWEEN 40 AND 60 DEG)

Chen. Helmet visor display employing reflective, refractive and diffractive optical components
US 5,526,183
Jun. 11, 1996

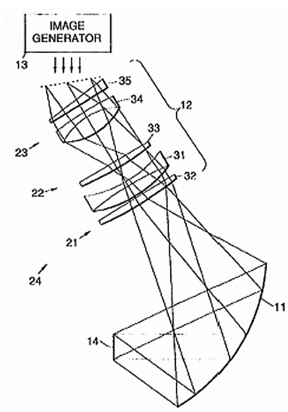

(a)

Chen. Wide spectral bandwidth virtual image display system.
US 5,436,763
Jul. 25, 1995

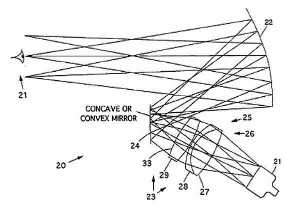

(b)

Chen. Ultra-wide field of view, broad spectral band visor display optical system.
US 5,499,139
Mar. 12, 1996

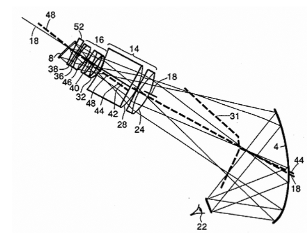

(c)

Takeyama. Image display apparatus.
US 6,342,871
Jan. 29, 2002

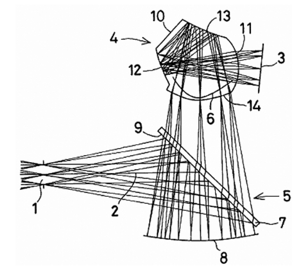

(d)

Togino. Visual display apparatus
US 5,436,765
Jul. 25, 1995

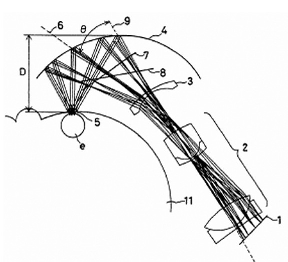

(e)

Becker. Head Mounted Display for Minian Video Display System.
US 5,003,300
Mar. 26, 1991

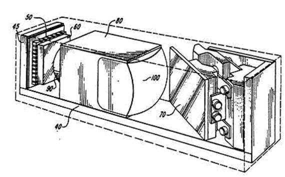

(f)

Erfle. Ocular.
US 1,478,704
Dec. 25, 1923

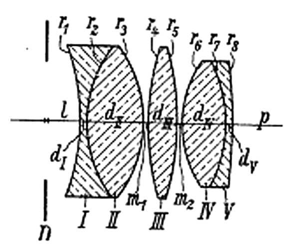

(g)

Several researchers are exploring the applications of HWDs in various fields. To date, HWDs have been used in applications such as supporting human memory [141], [153], future machine tools [143], factory automation [142], computer-supported collaborative work [144], personal imaging [145], telemedicine [146], urban environment guides [147], remote collaboration [148], computer games [149], [150], [156], archeological sites [151], [157], astronaut extravehicular activity [152], and medical applications [155]. A survey of augmented reality technology between 1997 and 2001, containing information on displays, new tracking sensors and applications, calibration and autocalibration, interfaces and visualization components and application can be found in [161].

Even though the markets might be driven initially by vertical applications, such as training, maintenance, manufacturing, and medical, we believe that it is the more horizontal adoption that will embed HWDs into societies around the world. In this low FOV regime, most of the HWD applications are expected to target mobile users. As the Lagrange invariant is relatively low compared to regimes with higher FOVs [63], the designs are likely to have a lower element count leading to potentially wearable, compact and lightweight displays with acceptable image quality.

Table I presents a collection of optical designs reasonably representative of HWDs in the low FOV regime that aim to fit to the eyeglass formfactor. In terms of the number of elements, designs fall between anywhere from one and six elements. Majority of these designs are within the one to three element(s) range, and laid out in off-axis geometries. Off-axis geometries can be desirable for conforming to the shape of the human head. All of the designs shown in Table II are catadioptric, except one HWD which makes use of a holographic element. An important metric is the value of the MTF at the Nyquist cut-off frequency given as $1/(2 * \text{pixel spacing})$. Typically a designer would aim at an as-built MTF value of 20% at the Nyquist cut-off frequency. The as-built MTF accounts for degradations imposed by optical and optomechanical tolerances. The spatial frequency corresponding to 50% MTF value is typically selected to ana-

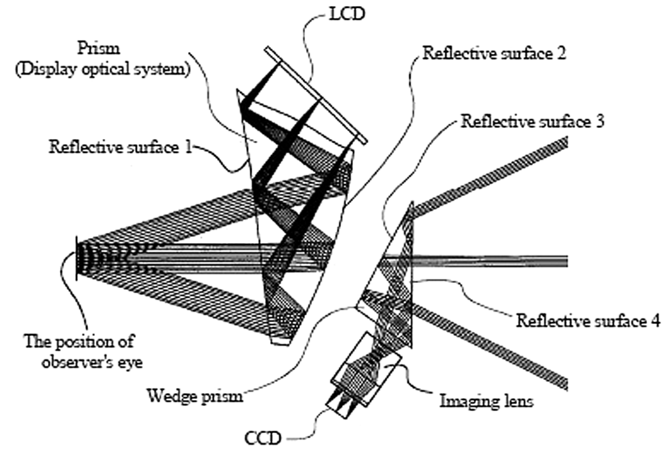

Fig. 5. Canon video seethrough system. (Adapted from [159]).

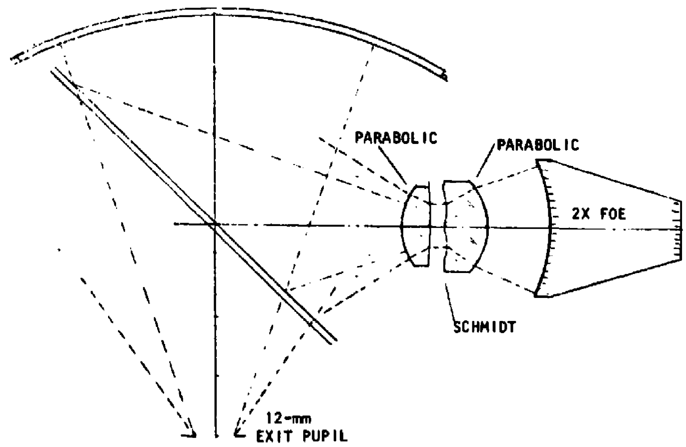

Fig. 6. Visually coupled airborne systems simulator (VCASS). (Adapted from [158]).

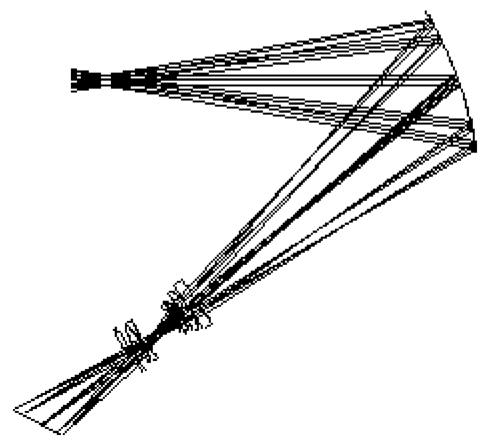

Fig. 7. Example rotationally symmetric high-FOV system. (Adapted from [39]).

lyze the robustness of the system to tolerances. Tolerances are determined by typically allowing an overall drop in MTF performance of less than 15%. Another metric that can differentiate these designs is the required number of compensators (i.e., adjustable groups or elements at system assembly) required to meet the as-built MTF specification. If a design is sensitive to positioning during the assembly phase, it will impose tight tolerances and additional optomechanical mechanisms will be necessary which add to the volume, weight and complexity of the overall design. It is desirable to have loose tolerances which allow for simpler optomechanical arrangements.

VII. Applications of HWDs: Mid-FOV Designs (Between 40 and 60 deg)

In this regime, example applications target scientific visualization, simulation and training, and medical training [160]. Table III provides seven designs each having between 40- and 60-deg FOV.

The Canon Mixed Reality Laboratory has developed a hybrid HWD with a camera that is able to record the FOV the user is looking at and can operate in see-through mode simultaneously. The freeform prism designed by Yamazaki *et al.*[159] successfully folds the optical path in a compact package. The optical layout one of the prototypes is shown in Fig. 5. The "COASTAR" HWD has a 60-deg diagonal FOV, 12-mm exit pupil diameter, 20-mm eye relief. The total thickness of the prism was reported to be 17.9 mm. The image plane was placed at 2 m.

VIII. Applications of HWDs: Wide FOV Designs ($>$ 60 deg)

Wide FOV designs are potentially applicable for applications requiring immersion such as simulation and training and computer games.

Buchroeder [158] designed a 48.5 deg$\times$56.5 deg per eye with a 15-deg overlap and achieved a 102-deg image. The design is reported to have a 12-mm exit pupil and 55-mm eye relief. In terms of collimation, divergence is 15 arcmins, divergence is 40 arcmins and convergence is 25 arcmins. Distortion of the design was specified to be $\pm 1\%$. Color correction across 486–656 nm was reported to be less than 1 arcmins for axial color and less than 3 arcmins for lateral color. The final design is an achromatized version of the layout shown in Fig. 6. The fiber optic faceplate shown in Fig. 6 was eliminated in the final design in exchange of a field flattening single lens element.

A classic and compact design in this regime is the Pancake window [110]. In the original system a single curved, spherical beamsplitting mirror was used as the image-forming element. More compact Pancake windows have since been designed using holographic combiners. The Pancake window is based on polarization optics and the original version has a very low light throughput at about 1%. Using cholesteric liquid crystals, the light throughput of the original Pancake window has been improved to 20% [111]. The HWDs, based on cholesteric liquid crystal type Pancake windows, have been built in tiled configurations, providing an FOV about 100 deg horizontal by 30 deg vertical. Later versions of the tiled Pancake windows are reported to reach fields of view of about 50 deg by 150 deg with 4 arcmins resolution [33].

Using nodal aberration theory, one can predict that the astigmatism and coma from the tilted combiner can be corrected by a rotationally symmetric, but tilted, optical system. This idea was employed in the system shown in Fig. 7 to achieve a high FOV

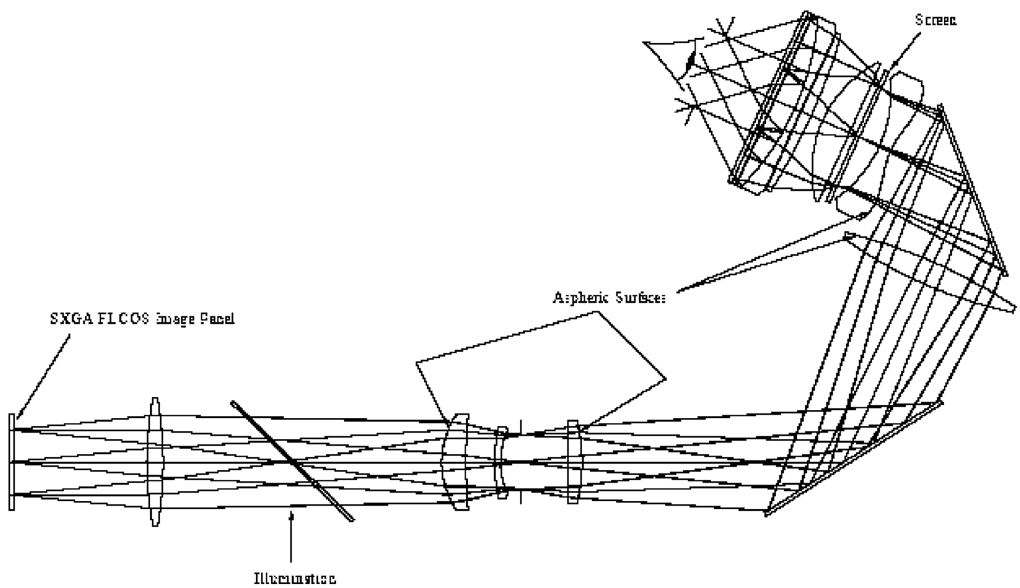

Fig. 8. An example wide field of view system (120° × 67°).

(100° × 50°) rotationally symmetric system with a 50-mm eye relief and a 15-mm exit pupil size. Rotational symmetry leads to ease of fabrication. Writings of Thompson [40] and Rodgers [11] provide fundamentals towards understanding nodal aberration theory and its application to tilted and decentered systems.

Rodgers [108] discusses the benefits of using freeform surfaces in order to reduce astigmatism from oblique rays. Astigmatism will be reduced dramatically, for example, for a single surface, broken into local patches, in the case where each patch is symmetric from the point of view of the chief ray of the beam hitting the patch. As ray-trace codes adopt tools and metrics to evaluate the degree of difficulty for manufacturing a surface, we can expect the newer HWD designs to utilize more free-form optics. The magnitude of the sag of a non-rotationally symmetric surface has been proposed as a metric to quantify the degree of fabrication difficulty [109]. The authors note that each process would have a unique cost function, thus, until general and flexible metrics are in place characterizing different processes, the authors chose not to implement this single metric in their ray-trace code for the time being.

Huxford designed a 120° × 67° FOV display for a low-cost driving simulation application [80]. The system has a 15-mm eye relief, 20-mm exit pupil, $\leq 0.25\%$ distortion, ±4 D focus adjustment, and a pixel-limited resolution of less than 4 arcminutes. The optical layout of this system is shown in Fig. 8. Huxford was using an FLCOS as the microdisplay. However, this is compensated for in the relay lenses. The eyepiece in this design was based on the Pancake window.

The polarizers in the system were utilizing wire-grid technology. The eyepiece had $> 27\%$ distortion. In order to achieve 50-lp/mm resolution across the FOV and the weight target, the author was using a combination of plastic and glass materials. The relay is composed of six lenses, four polymer lenses each having an aspherical surface and two glass lenses with spherical surfaces. The strong aspheres close to the screen help with distortion correction. The authors also designed an all polymer relay and they report that the hybrid relay performed 33% better in terms of the transverse color correction.

IX. Conclusion and Future Research Directions

We presented a review of state-of-the-art HWD design, focusing on the optical engineering and human perception aspects. Based on the complexity trade-offs of such designs, HWDs should be tailored for each application. A key difference in the optical design of HWDs compared to other areas of optical design is that imperfections can be tolerated (e.g., HWD design does not aim for diffraction-limited designs), within the aberration tolerances of the eye and perhaps even more as needed by the application requirements.

From the users perspective, we summarized important parameters such as the FOV, microdisplays, luminance and contrast, tradeoffs in HWDs, modes of operation followed by a summary of the human visual system parameters related to HWDs. From the optical designers perspective, we surveyed only a subset of all suitable and possible designs. Most practicing optical designers would use references compiling several optical system designs or commercially available electronic patent databases as a starting point for their design.

Generalized criteria and tools in the form of ray-trace code macros are available that allow for assessing HWDs in visual space. Suggested criteria for visual assessment include the modulation transfer function in cycles/arcminute, astigmatism in both diopters and arcminutes, shift in accommodation in diopters and the transverse color smear in arcminutes [68], [95].

We believe that there are opportunities for research in terms of refining models for depth perception in HWDs. Current models have assumed planes mapping to planes and have defined zero disparity based on the image plane of the microdisplay as opposed to the geometric or perceptual horopter. We should note other factors such as the viewing distance (i.e, distance scaling of disparity information) and how context affects depth perception. The consequences of these assumptions need to be assessed in detail which will be critical for applications having accurate depth perception requirements. Future perception studies on binocular rivalry in see-through monocular displays would enrich the literature improving our understanding of these devices. Further foreseeable opportunities in HWD design include the development of multi-focal plane capability, eye-tracking integration, application of micro-lenslet arrays to illumination [94], and compact optical designs that support mutual occlusion.

Acknowledgment

The authors would like to thank H. Urey for informative discussion on RSD technology; J. McGuire and J. Rogers for providing information related to their recent work as well as sharing their searches on the prior art of HMD design; and G. de Wit and S. Yamazaki for their insightful comments. They also thank K. Thompson and R. Patterson for reviewing the optics and perception aspects of the manuscript, respectively, and S. Feiner and J. Melzer for stimulating discussions on the use of the term head-worn display versus head-mounted display.

References

[1] H. Urey, "Spot size, depth-of-focus, and diffraction ring intensity formulas for truncated Gaussian beams," *Appl. Opt.*, vol. 43, no. 3, pp. 620–625, Jan. 2004.

[2] V. Mahajan, *Optical Imaging and Aberrations*. Bellingham, WA: SPIE Press, 2001.

[3] R. Draper, M. Wood, B. Radmard, K. Mahmud, P. Schuler, G. A. Sotzing, V. Seshadri, W. Mino, J. Padilla, and T. F. Otero, D. G. Hopper, E. W. Forsythe, D. C. Morton, C. E. Bradford, and H. J. Girolamo, Eds., "Electrochromic variable transmission optical combiner," in *Proc. SPIE*, May 2005, vol. 5801, Cockpit and Future Displays for Defense and Security, pp. 268–277.

[4] R. H. Webb, G. W. Hughes, and O. Pomerantzeff, "Flying spot TV opthalmoscope," *Appl. Opt.*, vol. 19, pp. 2991–2997, 1980.

[5] D. Holmgren and W. Robinett, "Scanned laser displays for virtual reality: A feasibility study," *Presence*, vol. 2, pp. 171–184, 1993.

[6] G. C. de Wit, "A retinal scanning display for virtual reality," Ph.D., Techn. Univ. Delft, Delft, The Netherlands, 1997.

[7] G. De Vos and G. Brandt, R. J. Lewandowski, Ed., "Use of holographic optical elements in HMDs," in *Proc. SPIE*, Oct. 1990, vol. 1290, Helmet Mounted Displays II.

[8] J. A. Cox, T. A. Fritz, and T. Werner, R. J. Lewandowski, W. Stephens, and L. A. Haworth, Eds., "Application and demonstration of diffractive optics for head-mounted displays," in *Proc. SPIE*, Jun. 1994, vol. 2218, Helmet- and Head-Mounted Displays and Symbology Design Requirements.

[9] P. Twardowski and P. Meyrueis, H. M. Assenheim, R. A. Flasck, T. M. Lippert, and J. Bentz, Eds., "Design of an optimal single reflective holographic helmet display element," in *Proc. SPIE Large Screen Projection, Avionic, and Helmet-Mounted Displays*, Aug. 1991, vol. 1456.

[10] Welch, "Diffractive optics for head-mounted displays," in *Proc. SPIE*, 1995, vol. 2409, Stereoscopic Displays and Virtual Reality Systems II, pp. 209–210.

[11] J. R. Rogers, Rogers and Fischer, Eds., "Aberrations of optical systems with large tilts and decentrations," in *Proc. SPIE*, 1983, vol. 0399, Optical System Design, Analysis, and Production.

[12] M. J. Hayford, Fischer, Price, and Smith, Eds., "Optical system design using holographic optical elements," in *Proc. SPIE*, 1985, vol. 0531, Geometrical Optics.

[13] P. J. Rogers, Taylor and Moore, Eds., "Biocular magnifiers—A review," in *Proc. SPIE 1985 Int. Lens Design Conf.*, 1985, vol. 0554.

[14] W. C. Sweatt, "Describing holographic optical elements as lenses," *J. Opt. Soc. Amer.*, vol. 67, no. 6, pp. 803–808, Jun. 1977.

[15] D. Faklis and M. J. Hoppe, "Effects of diffraction on the performance of diffractive realy optics," in *Proc. SPIE*, 1994, vol. 2218, Head-Mounted Displays and Symbology Design Requirements, pp. 32–40.

[16] M. L. Thomas, "Fiber optic development for use on the fiber optic helmet mounted display," in *Proc. SPIE*, 1989, vol. 1116, Helmet- and Head-Mounted Displays and Symbology Design Requirements, pp. 89–95.

[17] D. F. Kocian, Armstrong Aerospace Medical Res. Lab., Visual Display Sytems Branch, Wright-Patterson Air Force Base, Dayton, OH, "Design considerations for virtual panoramic display (VPD) helmet systems", 1988.

[18] Scidmore and Flanagan, "Wide angle eyepiece with large eye relief," U.S. Patent 3 384 434, May 21, 1968.

[19] Dilworth, "Extreme Wide Angle Eyepiece with Minimal Aberrations," U.S. Patent 4 720 183, Jan. 19, 1988.

[20] M. Kidger, *Fundamentals of Optical Design*. Bellingham, WA: SPIE, 2001, pp. 26–27.

[21] R. G. Collier, *Optical Holography*. Orlando, FL: Academic, 1971.

[22] D. A. Buralli and G. M. Morris, "Effects of diffraction efficiency on the modulation transfer function of diffractive lenses," *Appl. Opt.*, vol. 31, no. 22, pp. 4389–4396, Aug. 1992.

[23] J. Rolland, Y. Ha, and C. Fidiopiastis, "Albertian errors in head-mounted displays: I. Choice of eye-point location for a near- or far-field task visualization," *J. Opt. Soc. Amer. A*, vol. 21, no. 6, pp. 901–1118, Jun. 2004.

[24] D. Williamson, Fischer, Price, and Smith, Eds., "The eye in optical systems," in *Proc. SPIE*, Jan. 1985, vol. 0531, Geometrical Optics, pp. 136–147.

[25] W. N. Charman, , Bass, Ed., "Optics of the eye," in *Handbook of Optics*, 2nd ed. New York: McGraw-Hill, 1995, vol. 1.

[26] Katz and Zikos, "Apparent image quality of magnifiers depends on amplitude of accommodation," *Optom. Vis. Sci.*, vol. 71, pp. 226–234, 1994.

[27] G. A. Fry, , Kingslake, Ed., "The eye and vision," in *Applied Optics and Optical Engineering*R. Kingslake, Ed., 2nd ed. New York: Academic, 1965, vol. II, pp. 2–26.

[28] Williams and Coletta, "Cone spacing and the visual resolution limit," *J. Opt. Soc. Amer. A*, vol. 4, no. 8, 1987.

[29] C. A. Curcio, K. R. Sloan, R. E. Kalina, and A. E. Hendrickson, "Human photoreceptor topography," *J. Comparative Neurol.*, vol. 292, pp. 497–523, 1990.

[30] U.S. Dep. of Defense, Washington, DC, *Military Handbook 141*, "Optical design," 1962.

[31] W. Knapp, G. Blough, K. Khajurivala, R. Michaels, B. Tatian, and B. Volk, "Optical design comparison of 60 degree eyepieces: One with a diffractive surface and one with aspherics," *Appl. Opt.*, vol. 36, no. 20, pp. 4756–4760.

[32] E. J. Ludvigh and J. W. Miller, "Study of visual acuity during the ocular pursuit of moving test objects: I. Introduction," *J. Opt. Soc. Amer.*, vol. 48, no. 1, pp. 799–802, 1958.

[33] J. E. Melzer, R. J. Lewandowski, L. A. Haworth, and H. J. Girolamo, Eds., "Overcoming the field of view: Resolution invariant in head mounted displays," in *Proc. SPIE*, Jul. 1998, vol. 3362, Helmet- and Head-Mounted Display III.

[34] W. Barfield and T. Caudell, Eds., *Fundamentals of Wearable Computers and Augmented Reality*. Mahwah, NJ: Lawrance Erlbaum, 2001.

[35] Tabata, "Display Apparatus to be Mounted on the Head or Face o fan Individual," U.S . Patent 5 726 670, Mar. 10, 1998.

[36] Y. Y. Yeh and L. D. Silverstein, "Limits of fusion and depth judgement in stereoscopic color displays," *Human Factors*, vol. 32, pp. 45–60, 1990.

[37] K. Moffit, , J. Melzer and K. Moffitt, Eds., *Designing HMDs for Viewing Comfort*. New York: McGraw-Hill, 1997, Head-mounted Displays: Designing for the User, pp. 117–142.

[38] J. Rolland, M. Krueger, and A. Goon, "Multifocal planes head-mounted displays," *Appl. Opt.*, vol. 39, no. 19, pp. 3209–3215, 2000.

[39] A. Sisodia, A. Riser, and J. R. Rogers, D. Hopper, E. Forsythe, D. Morton, C. Bradford, and H. Girolamo, Eds., "Design of an advanced helmet mounted display (AHMD)," in *Proc. SPIE*, May 2005, vol. 5801, Cockpit and Future Displays for Defense and Security, pp. 304–315.

[40] K. P. Thompson, "Aberration fields in tilted and decentered optical systems," Ph.D., Univ. Arizona, Tempe, 1980.

[41] H. Hua, Y. Ha, and J. P. Rolland, "Design of an ultra-light and compact projection lens," *Appl. Opt.*, vol. 42, pp. 97–107, 2003.

[42] G. Smith and D. A. Atchison, *The Eye and Visual Optical Instruments*. Cambridge, U.K.: Cambridge Univ. Press, 1997.

[43] R. Mortimer, A. L. Dyer, and J. R. Reynolds, "Electrochromic organic and polymeric materials for display applications," *Displays*, vol. 27, pp. 2–18, 2006.

[44] F. P. Shvartsman, , S. H. Lee, Ed., "Replication of diffractive optics," in *Diffractive and Miniatuzrized Optics*. Bellingham, WA: SPIE Critical Reviews of Optical Science and Technology, 1993, vol. CR49.
[45] A. Becker, "Miniature video display system," U.S. Patent 4 934 773, Jun. 19, 1990.
[46] E. Peli, "Visual issues in the use of a head-mounted monocular display," *Opt. Eng.*, vol. 29, no. 8, pp. 883–892, Aug. 1990.
[47] G. J. Burton and N. D. Haig, "Effects of the Seidel aberrations on visual target discrimination," *J. Opt. Soc. Amer. A*, vol. 1, no. 4, pp. 373–385, Apr. 1984.
[48] T. Stone and N. George, "Hybrid diffractive-refractive lenses and achromats," *Appl. Opt.*, vol. 27, no. 14, pp. 2960–2971, Jul. 1988.
[49] A. P. Wood, "Design of infrared hybrid refractive-diffractive lenses," *Appl. Opt.*, vol. 31, no. 13, pp. 2253–2258, May 1992.
[50] D. M. Green and J. A. Swets, *Signal Detection Theory and Psychophysics*. New York: Wiley, 1966.
[51] J. Wann, S. Rushton, and M. Mon-Williams, "Natural problems in the perception of virtual environments," *Vision Res.*, vol. 35, pp. 2731–2736, 1995.
[52] "Furness. Virtual Retinal Display," U.S. Patent 5 467 104, Nov. 14, 1995.
[53] H. Urey, "Vibration mode frequency formulae for micromechanical scanners," *J. Micromech. Microeng.*, vol. 15, pp. 1713–1721, 2005.
[54] H. Urey, "Retinal scanning displays," in *Encyclopedia of Optical Engineering*, R. Driggers, Ed. New York: Marcel Dekker, vol. 3, pp. 2445–2457.
[55] H. Urey, D. Wine, and J. Lewis, "Scanner design and resolution tradeoffs for miniature scanning desplays," in *Flat Panel Display Technology and Display Metrology, Proc. SPIE*, San Jose, CA, vol. 3636, pp. 60–68.
[56] H. C. Self, Optical tolerances for alignment and image differences for binocular helmet-mounted displays Armstrong Aerospace Medical Research Lab., Dayton, OH, 1986, AAMRL-TR-86-019.
[57] *"Helmet-Mounted Displays: Design Issues for Rotary-Wing Aircraft,"* C. Rash, Ed., U.S. Army Aeromedical Research Lab, Fort Rucker, AL, 2000.
[58] S. T. Wu, *Reflective Liquid Crystal Displays*. Hoboken, NJ: Wiley, 2001.
[59] R. Patterson and W. L. Martin, "Human stereopsis," *Human Factors*, vol. 34, no. 6, pp. 669–692, 1992.
[60] P. Mustillo, "Binocular mechanisms mediating crossed and uncrossed stereopsis," *Psychol. Bull.*, vol. 97, no. 2, pp. 187–201, 1985.
[61] C. M. Schor and I. Wood, "Disparity range for local stereopsis as a function of luminance spatial frequency," *Vision Res.*, vol. 23, no. 24, pp. 1649–1654, 1983.
[62] M. Rosete-Aguilar and J. L. Rayces, "Eye rotation and vignetting in visual instruments," *Appl. Opt.*, vol. 41, no. 31, pp. 6593–6602, Nov. 2002.
[63] J. Rogers, private communication. Feb. 2006.
[64] State, "Simulation-based design and rapid prototyping of a parallax-free, orthoscopic video see-through head-mounted display," in *Proc. Int. Symp. on Mixed and Augmented Reality (ISMAR)*, Vienna, Austria, 2005, pp. 28–31.
[65] I. E. Sutherland, "A head-mounted three-dimensional display," in *AFIPS Proc. Fall Joint Computer Conf.*, 1968, vol. 33, pp. 757–764.
[66] K. Kiyokawa, M. Billinghurst, B. Campbell, and E. Woods, "An occlusion-capable optical see-through head mount display for supporting co-located collaboration," in *Proc. Int. Symp. on Mixed and Augmented Reality (ISMAR)*, 2003, pp. 133–141.
[67] S. R. Ellis and U. J. Bucher, "Distance perception of stereoscopically presented virtual objects optically superimposed on physical objects in a head-mounted see-through displays," in *Proc. Human Factors and Ergonomic Soc.*, Nashville, TN, 1994.
[68] M. Shenker, G. Forbes, Ed., "Image quality considerations for head-mounted displays," in *Int. Optical Design Conf.*, 1994, vol. 22.
[69] B. T. Schowengerdt and E. J. Seibel, "True 3D displays that allow viewers to dynamically shift accommodation, bringing objects displayed at different viewing distances into and out of focus," *CyberPsychology & Behavior*, vol. 7, no. 6, pp. 610–620, 2004.
[70] Manhart, "Augeye: A compact, solid, schmidt optical relay for helmet mounted applications," in *Proc. IEEE VRAIS '93*, pp. 234–245.
[71] R. Kojima and T. Ojika, "Transition between virtual environment and workstation environment with projective head-mounted display," in *Proc. VRAIS '97*, pp. 130–137.
[72] O. Bimber and R. Raskar, *Spatial Augmented Reality*. Wellesley, MA: Peters, 2005.
[73] Watanabe, "A retinal scanning display with a wavefront curvature modulator," *J. Soc. Inf. Display*, vol. 11, no. 511, 2003.
[74] C. Pinhanez, "The everywhere displays projector: A device to create ubiquitous graphical interfaces," in *Proc. 3rd Int. Conf. on Ubiquitous Computing*, Berlin, 2001, vol. 2201, Lecture Notes in Computer Science, pp. 315–331.
[75] G. C. de Wit, "Retinal scanning displays: Light sources moving over the retina," *Sci. Progr.*, vol. 82, pp. 135–149, 1999.
[76] ——, "Contrast of displays on the retina," *J. Soc. Inf. Display*, vol. 13, pp. 178–179, 2005.
[77] G. C. de Wit, private communication. Feb. 2006.
[78] Starner, "Augmented reality through wearable computing," *Presence*, vol. 6, no. 4, 1997.
[79] R. E. Jacobson, , Kinglake, Ed., "Projection screens," in *Applied Optics and Optical Engineering*. New York: Academic, 1965, vol. I, ch. 10.
[80] R. B. Huxford, L. Mazuray, P. J. Rogers, and R. Wartmann, Eds., "Wide FOV head mounted display using hybrid optics," in *Proc. Optical Design and Engineering*, 2004, vol. 5249.
[81] T. M. Aye, R. J. Lewandowski, L. A. Haworth, H. J. Girolamo, and C. E. Rash, Eds., "Compact HMD optics based on multiplexed aberration compensated holographic optical elements," in *Proc. SPIE Helmet- and Head-Mounted Display VI*, 2001, vol. 4361.
[82] J. E. Melzer, R. J. Lewandowski, L. A. Haworth, H. J. Girolamo, and C. E. Rash, Eds., "Design evolution of a wide field of view head-mounted display for aircraft training and simulation," in *Proc. SPIE Helmet- and Head-Mounted Display VI*, 2001, vol. 4361.
[83] F. J. Ferrin, "An update on optical systems for military head mounted displays," in *Proc. SPIE Helmet- and Head-Mounted Display IV*, Orlando, FL, Apr. 1999, pp. 178–185.
[84] Ando, "Head mounted display using holographic optical element," in *Proc. SPIE*, 1998, vol. 3293, pp. 183–189.
[85] K. Keller and D. Colucci, "Perception in HMDs: What is it in head mounted displays (HMDs) that really make them all so terrible?," in *Proc. SPIE Helmet- and Head-Mounted Display III*, Orlando, FL, 1998.
[86] Hoshi, M. Bolas, S. Fisher, and J. O. Merritt, Eds., "Off-axial HMD optical system consisting of aspherical surfaces without rotational symmetru," in *Proc. SPIE*, 1996, vol. 2653, Stereoscopic Displays and Virtual Reality Systems III, pp. 234–242.
[87] D. Colucci and V. Chi, J. M. Sasian, Ed., "Computer glasses: A compact, light weight and cost effective display for monocular and tiled wide field of view systems," in *Proc. SPIE*, vol. 2537, Novel Optical Systems Design and Optimization, pp. 61–70.
[88] J. S. Kollin and M. Tidwell, J. M. Sasian, Ed., "Optical engineering challenges of the virtual retinal display," in *Proc .SPIE*, vol. 2537, Novel Optical Systems Design and Optimization, pp. 48–60.
[89] Bauer, T. D. Goodman, Ed., "Optical coatings on polymers. Advancements in polymer optics design, fabrication and materials," in *Proc. SPIE*, vol. 5872.
[90] G. Kelly, M. Shenker, and P. Weissman, T. M. Lipper, Ed., "Helmet-mounted area of interest," in *Proc. SPIE*, 1992, vol. 1695, Helmet-Mounted Display III, pp. 58–63.
[91] R. A. Buchroeder, J. Sasian, Ed., "Distortion correction for oblique projection onto a curved screen," in *Proc. SPIE*, 1995, vol. 2537, Novel Optical Systems Design and Optimization, pp. 96–104.
[92] J. E. Melzer, D. G. Hopper, E. Forsythe, D. C. Morton, C. E. Bradford, and H. J. Girolamo, Eds., "Integrated headgear for the future force warrior and beyond," in *Proc. SPIE*, 2005, vol. 5801, Cockpit and Future Displays for Defense and Security, pp. 173–178.
[93] Y. Ha, V. Smirnov, L. Glebov, and J. Rolland, C. E. Rash and C. E. Reese, Eds., "Optical modeling of a holographic single-element head-mounted display," in *Proc. SPIE*, 2004, vol. 5442, Helmet- and Head-Mounted Displays IX: Technologies and Applications, pp. 254–260.
[94] V. Shaoulov, R. Martins, and J. Rolland, C. E. Rash and C. E. Reese, Eds., "Magnifying miniature displays with microlenslet arrays", in *Helmet- and Head-Mounted Displays IX: Technologies and Applications.* 2004.
[95] Y. Ha and J. Rolland, "Optical assessment of head-mounted displays in visual space," *Appl. Opt.*, vol. 41, no. 25, pp. 5282–5289, 2002.
[96] K. M. Robinette, "Anthropometry for HMD design," in *Proc. SPIE Aerosense*, 1992, vol. 1695, Helmet Mounted Displays III, pp. 138–145.
[97] Lippert, "Fundamental monocular/binocular HMD human factors," in *Proc. SPIE*, 1990, vol. 1290, Helmet-mounted displays II, pp. 185–191.
[98] Howlett, "Wide angle orthostereo," in *Proc. SPIE*, 1990, vol. 1256, Stereoscopic Displays and Applications, pp. 210–223.
[99] D. Faklis and G. M. Morris, "Diffractive optics technology for display applications," in *Proc. SPIE*, 1995, vol. 2407, pp. 57–61.

[100] Y. Wang, L. Li, and Q. Xin, “Optical design and fabrication in China,” in *Int. Optical Design Conf.*, 2002.
[101] P. J. Rogers, W. J. Smith, Ed., “The optics/vision interface,” in *Proc. Critical Rev.*, Jan. 1992, vol. CR41, Lens Design.
[102] P. Mouroulis, K. Lyons, and G. Zhao, R. E. Fischer and W. J. Smith, Eds., “Aberrration balancing in the design of visually coupled lens systems,” in *Proc. SPIE*, Nov. 1993, vol. 2000, Current Developments in Optical Design and Optical Engineering III.
[103] R. R. Willey and M. E. Durham, G. N. Lawrence, Ed., “Ways that designers and fabricators can help each other,” in *Proc. SPIE 1990 Int. Lens Design Conf.*, Jan. 1991, vol. 1354.
[104] D. Armitage, I. Underwood, and S. T. Wu, *Introduction to Microdisplays*. Hoboken, NJ: Wiley, 2005.
[105] M. Hoppe and J. Melzer, “Optical tiling for wide field-of-view head-mounted displays,” in *Proc. SPIE Conf. on Current Developments in Optical Design and Optical Engineering VIII*, Denver, CO, 1999.
[106] A. Yoshida, J. P. Rolland, and J. H. Reif, “Design and applications of a high-resolution insert head-mounted display,” in *Proc. 1995 Virtual Reality Annual Int. Symp.*, Mar. 1995, pp. 84–93.
[107] D. Hasenauer and J. Kunick, “Full field mapping and analysis of veiling glare sources for helmet mounted display systems,” in *Proc. SPIE Conf. on Current Developments in Optical Design and Optical Eng. VIII*, Denver, CO, 1999.
[108] Rodgers and Thompson, “Benefits of freeform mirror surfaces in optical design,” in *Proc. Amer. Soc. for Precision Eng.*, 2004.
[109] K. Garrard, T. Bruegge, J. Hoffman, T. Dow, and A. Sohn, P. Mouroulis, W. Smith, and B. Johnson, Eds., “Design tools for freeform optics,” in *Proc. SPIE Current Developments in Lens Design and Optical Engineering VI*, 2005, vol. 5874.
[110] J. A. La Russa, “Image forming apparatus,” U.S. Patent 3 940 203, Feb. 24, 1976.
[111] A. L. Berman and J. E. Melzer, “Optical collimating apparatus,” U.S. Patent 4 859 031, Apr. 22, 1989.
[112] M. A. Karim, *Electro-Optical Displays*. New York: Marcel Dekker, 1992.
[113] Coulman and Petrie, “Some notes on the designing of aspherical magnifiers for binocular vision,” *J. Opt. Soc. Amer.*, vol. 39, no. 7, 1949.
[114] H. T. E. Hertzberg, G. S. Daniels, and E. Churchill, Antropometry of Flying Personnel Wright Air Development Center, Wright-Patterson Air Force Base, OH, WADC TR-52-321.
[115] A. Yalcinkaya, H. Urey, D. Brown, T. Montague, and R. Sprague, “Two-axis electromagnetic microscanner for high resolution displays,” *J. Microelectromech. Syst.*, 2006, to be published.
[116] W. Plummer, “Unusual optics of the polaroid SX-70 land camera,” *App. Opt.*, vol. 21, p. 196-, 1982.
[117] W. T. Plummer, J. G. Baker, and J. V. Tassell, “Photographic optical systems with nonrotational aspheric surfaces,” *Appl. Opt.*, vol. 38, pp. 3572–3592, 1999.
[118] F. Biocca and J. Rolland, “Virtual eyes can rearrange your body: Adaptation to visual displacement in see-through head-mounted displays,” *Presence*, vol. 7, no. 3, pp. 262–278, 1998.
[119] R. Patterson, L. Moe, and T. Hewitt, “Factors that affect depth perception in stereoscopic displays,” *Human Factors*, vol. 34, pp. 655–667, 1992.
[120] M. D. Missig and G. M. Morris, “Using diffractives in an eyepiece,” *Appl. Opt.*, vol. 34, no. 14, 1995.
[121] M. Velger, *Helmet-Mounted Displays and Sights*. Norwood, MA: Artech House, 1998.
[122] R. Patterson, M. Winterbottom, and B. Pierce, “Perceptual issues in the use of head-mounted visual displays,” *Human Factors*, to be published.
[123] K. N. Ogle and J. T. Schwartz, “Depth of focus of the human eye,” *J. Opt. Soc. Amer.*, vol. 49, pp. 273–280, 1959.
[124] R. T. Hennessy, T. Iida, K. Shina, and H. W. Leibowitz, “The effect of pupil size on accommodation,” *Vision Res.*, vol. 16, no. 6, pp. 587–589, 1976.
[125] C. A. Johnson, “Effects of luminance and stimulus distance on accommodation and visual resolution,” *J. Opt. Soc. Amer.*, vol. 66, pp. 138–142, 1976.
[126] A. Ivanoff, “Night binocular convergence and night myopia,” *JOSA*, vol. 45, pp. 769–770, 1955.
[127] M. S. Livingstone and D. H. Hubel, “Segregation of form, color, movement, and depth: Anatomy, physiology and perception,” *Science*, vol. 240, pp. 740–749, 1988.
[128] Angel, “Quantitative pupillometry: Normative data in healthy pediatric volunteers,” *J. Neurosurg*, vol. 103, pp. 496–500, 2005.
[129] D. G. McCauley, C. E. Simpson, and W. J. Murbach, “Holographic optical element for visual display applications,” *Appl. Opt.*, vol. 12, no. 2, 1973.
[130] W. A. Kleinhans, “Aberrations of curved zone plates and fresnel lenses,” *Appl. Opt.*, vol. 16, no. 6, 1977.
[131] W. J. Smith, *Modern Lens Design*, 2nd ed. New York: McGraw-Hill, 2005.
[132] W. Mandler, “Design of double Gauss lenses,” in *SPIE*, 1980, vol. 237, p. 222.
[133] T. Gold, “Visual disparity tolerances for head-up displays,” in *Electro-Optical System Design Conf.*, Anaheim, CA, 1971, pp. 399–406.
[134] T. Gold and A. Hyman, “Visual requirements for head-up displays,” Final Rep. Speery-Rand Corp., prepared for the Office of Naval Research, 1970, Phase 1. JANAIR report 680712.
[135] E. Tatham, “Getting the best of both real and virtual worlds,” *Commun. ACM*, vol. 42, no. 9, pp. 96–98.
[136] T. Uchida, K. Sato, and S. Inokuchi, “An optical see-through MR display with digital micro-mirror device,” *Trans. Virtual Reality Soc. Jpn.*, vol. 7, no. 2, 2002.
[137] O. Cakmakci, Y. Ha, and J. Rolland, “A compact optical see-through head-worn display with occlusion support,” in *Proc. Int. Symp. on Mixed and Augmented Reality (ISMAR)*, Arlington, VA, 2005.
[138] J. Sheedy and N. Bergstrom, “Performance and comfort on near-eye computer displays,” *Optom Vis Sci.*, vol. 79, no. 5, pp. 306–12, 2002.
[139] V. Mahajan, “Aberrations of diffracted wave fields. I. Optical imaging,” *JOSA A*, pp. 2216–2222, Dec. 2000.
[140] E. R. Kandel, J. H. Schwartz, and T. M. Jessell, *Essentials of Neural Science and Behavior*. New York: McGraw-Hill, 1997.
[141] B. Rhodes, “The wearable remembrance agent: A system for augmented memory,” in *Proc. Int. Symp. on Wearable Computers (ISWC)*, Boston, MA, 1997, p. 123.
[142] C. Thompson, “Factory automation support technology (FAST),” in *Proc. Int. Symp. on Wearable Computers (ISWC)*, Boston, MA, 1997, p. 31.
[143] Daude, “Mobile approach support system for future machine tools,” in *Proc. Int. Symp. on Wearable Computers (ISWC)*, Boston, MA, 1997, p. 24.
[144] M. Billinghurst, “Wearable computers for three dimensional CSCW,” in *Proc. Int. Symp. on Wearable Computers (ISWC)*, Boston, MA, 1997, p. 39.
[145] S. Mann, “An historical account of ’WearComp’ and ’Wearcam’ inventions developed for applications in ’Personal Imaging’,” in *Proc. Int. Symp. on Wearable Computers (ISWC)*, Boston, MA, 1997, p. 66.
[146] A. P. Pentland, “The digital doctor: An experiment in wearable telemedicine,” in *Proc. Int. Symp. on Wearable Computers (ISWC)*, Boston, MA, 1997, p. 173.
[147] S. Feiner, “A touring machine: Prototyping 3D mobile augmented reality systems for exploring the urban environment,” in *Proc. Int. Symp. on Wearable Computers (ISWC)*, Boston, MA, 1997, p. 74.
[148] M. Bauer, “A collaborative wearable system with remote sensing,” in *Proc. Int. Symp. on Wearable Computers (ISWC)*, Pittsburgh, PA, 1998, p. 10.
[149] B. Thomas, “ARQuake: An outdoor/indoor augmented reality first person application,” in *Proc. Int. Symp. on Wearable Computers (ISWC)*, Atlanta, GA, 2000, p. 139.
[150] Y. Ohta and H. Tamura, *Mixed Reality: Merging Real and Virtual Worlds*. Secaucus, NJ: Springer-Verlag, 1999.
[151] V. Vlahakis, “Personalized augmented reality touring of acheological sites with wearable and mobile computers,” in *Proc. Int. Symp. on Wearable Computers (ISWC)*, Seattle, Washington, 2002, p. 15.
[152] C. Carr, “A wearable computer for support of astronaut extravehicular activity,” in *Proc. Int. Symp. on Wearable Computers (ISWC)*, Seattle, WA, 2002, p. 23.
[153] T. Kawamura, “Wearable interfaces for a video diary,” in *Proc. Int. Symp. on Wearable Computers (ISWC)*, Seattle, WA, 2002, p. 3.
[154] Y. Baillot, J. Rolland, K. Lin, and D. Wright, “Automatica modeling of knee-joint motion for the virtual reality dynamic anatomy (VRDA) tool,” *Presence*, vol. 9, no. 3, pp. 223–235, 2000.
[155] D. F. Ormerod, “Use of a see-through head-worn display of patient monitoring data to engance anesthesiologists’response to abnormal clinical events,” in *Proc. Int. Symp. on Wearable Computers (ISWC)*, Seattle, WA, 2002, p. 131.
[156] A. D. Cheok, “Game-city: A ubiquitous large area multi-interface mixed reality game space for wearable computers,” in *Proc. Int. Symp. on Wearable Computers (ISWC)*, Seattle, WA, 2002, p. 156.
[157] J. Cross, “Layered annotations of digital images for data collection in the field,” in *Proc. Int. Symp. on Wearable Computers (ISWC)*, White Plains, NY, 2003, p. 154.

[158] R. A. Buchroeder, G. W. Seeley, and D. Vukobratovich, "Design of a catadioptric vcass helmet-mounted display," Final Report Optical Sciences Center, University of Arizona, under contract to U.S. Air Force Armstrong Aerospace Medical Res. Lab., Wright-Patterson Air Force Base, Dayton, OH, AFAMRL-TR-81-133.

[159] A. Takagi, S. Yamazaki, Y. Saito, and N. Taniguchi, "Development of a stereo video see-through HMD for AT systems," in *Int. Symp. on Augmented Reality*, Munich, Germany, Oct. 5–6, 2000.

[160] Y. Argotti, L. Davis, V. Outters, and J. Rolland, "Dynamic superimposition of synthetic objects on rigid and simple-deformable real objects," *Computers & Graphics*, vol. 26, no. 6, pp. 919–930, 2002.

[161] R. Azuma, Y. Baillot, R. Behringer, S. Feiner, S. Julier, and B. MacIntyre, "Recent advances in augmented reality," *IEEE Comput. Graphics Appl.*, vol. 21, no. 6, pp. 34–47, 2001.

[162] P. Mouroulis, T. G. Kim, and G. Zhao, "Transverse color tolerances for visual optical systems," *Appl. Opt.*, vol. 32, no. 34, 1993.

[163] M. Reiss, "The $\cos^4$ law of illumination," *J. Opt. Soc. Amer.*, vol. 35, no. 4, pp. 283–288, 1945.

[164] Martins, "Head-mounted display by integration of phase-conjugate material," U.S. Patent 6 999 239, Feb. 14, 2006.

[165] Harvey, "Aberrations of diffracted fields: Distortion," *Appl. Opt.*, vol. 42, no. 7, pp. 1167–74, 2003.

[166] Vaissie, "head mounted display with eyetracking capability," U.S. 6 433 760, Aug. 13, 2002.

[167] J. Rolland and H. Hua, "Displays: Head-mounted," in *Encyclopedia of Optical Engineering*. New York: Marcel Dekker, 2005.

[168] C. Curatu, J. M. Sasian, R. J. Koshel, and R. C. Juergens, Eds., "Projection-based head-mounted display with eye tracking capabilities," in *Proc. SPIE Novel Optical Systems Design and Optimization VIII*, Aug. 2005, vol. 5875, pp. 141–149.

[169] J. P. Rolland, "Towards quantifying depth and size perception in virtual environments," *Presence*, vol. 4, no. 1, pp. 24–49, 1995.

[170] J. P. Rolland, "Method of adjustments versus method of constant stimuli in the quantification of accuracy and precision of rendered depth in head-mounted displays," *Presence*, vol. 11, no. 6, pp. 610–625, Dec. 2002.

[171] E. H. Stupp and M. S. Brennesholtz, *Projection Displays*. New York: Wiley, 1999.

[172] D. Burr, "Motion smear," *Nature*, vol. 284, pp. 164–165, Mar. 1980.

[173] R. Patterson, private communication. May 7, 2006.

[174] ——, "Spatiotemporal properties of stereoacuity," *Optom. and Vision Sci.*, vol. 67, pp. 123–128, 1990.

[175] R. H. Cormack, "Stereoscopic depth perception at far viewing distances," *Perception & Psychophys.*, vol. 35, pp. 423–428, 1984.

[176] R. Patterson and R. Fox, "The effect of testing method on stereoanomaly," *Vision Res.*, vol. 24, no. 5, pp. 403–408, 1984.

[177] S. Becker, C. Bowd, S. Shorter, K. King, and R. Patterson, "Occlusion contributes to temporal processing differences between crossed and uncrossed stereopsis in random-dot displays," *Vision Res.*, vol. 39, no. 2, pp. 331–339, 1999.

Ozan Cakmakci (S'04) is born in Ankara, Turkey. He received the B.S. degree in electrical engineering from Michigan State University, East Lansing, MI, in 1999, the M.S. degree in optics from the University of Central Florida, Orlando, FL, in 2004, and is currently working toward the Ph.D. degree with Jannick Rolland. His focus is on the optical design of eyeglass based displays and wearable augmented reality displays with mutual occlusion capability.

He has held an internship position, worked, or consulted for Optical Research Associates, Pasadena, CA; Human Computer Interaction Group, Institute Mathematique Applique de Grenoble, Grenoble, France; Epson Research & Development, Barcelona, Spain; Starlab Research N.V./S.A, Brussels, Belgium and Barcelona, Spain; BMW A.G. *Forschungs- und Innovationszentrum*, Munich, Germany. During the summer of 2006 he was with Canon Research Labs, Tokyo, Japan. He has co-invented 3 patents (2 pending) and coauthored a book chapter on augmented and virtual reality.

Mr. Cakmakci has received the 2005 Michael Kidger Memorial Award in Optical System Design.

Jannick Rolland (A'96) was born in Africa and raised in Europe. She received a Diploma from the Ecole Supérieure D'Optique in France in 1984, and the Ph.D. degree in optical science from the University of Arizona in 1990.

She is currently Associate Professor of optics, computer science, electrical engineering, and modeling and simulation at the University of Central Florida (UCF). She joined the Department of Computer Science at the University of North Carolina (UNC) at Chapel Hill as a Postdoctoral Fellow to conduct research in optical design for 3-D medical visualization. She was appointed Research Faculty at UNC in 1992 and headed the Vision Research Group from 1992 to 1996. She holds 11 patents, wrote 6 book chapters, and has over 50 peered review publications related to optical design, augmented reality, vision, and image quality assessment for medical imaging. She authored and coauthored over 100 other publications related to the same topics.

Dr. Rolland is on the editorial board of the *Journal Presence* (MIT Press) since 1996, and has been Associate Editor of *Optical Engineering* from 1999 to 2004. She is a Fellow of the Optical Society of America, and a member of SPIE and SID.